Decomposing the Tea Bag Index and finding slower organic matter loss rates at higher elevations and deeper soil horizons in a minerogenic salt marsh.

Satyatejas G. Reddy[1], W. Reilly Farrell[1], Fengrun Wu[2], Steven C. Pennings[3], Jonathan Sanderman[4], Meagan Eagle[5], Christopher Craft[6], Amanda C. Spivak[1]*

[1]University of Georgia, Marine Sciences Department, Athens, GA, USA 30602
[2]Xiamen University of Technology, School of Environmental Science and Engineering, Xiamen, Fujian Province, China
[3]University of Houston, Department of Biology and Biochemistry, Houston TX 77204, USA
[4]Woodwell Climate Research Center, Falmouth, MA, USA
[5]United States Geological Survey, Marine Science Center, Woods Hole, MA, USA
[6]Indiana University Bloomington, School of Public and Environmental Affairs, Bloomington IN 47405, USA
*corresponding author: aspivak@uga.edu

Keywords: decay, decomposition, salt marsh, organic matter, Tea Bag Index, hydrology
Running title: TBI and organic matter decay in marshes

Abstract

Environmental gradients can affect organic matter decay within and across wetlands and contribute to spatial heterogeneity in soil carbon stocks. We tested the sensitivity of decay rates to tidal flooding and soil depth in a minerogenic salt marsh using the Tea Bag Index (TBI). Tea bags were buried at 10 and 50 cm depths across an elevation gradient in a subtropical *Spartina alterniflora* marsh in Georgia (USA). Plant and animal communities and soil properties were characterized once while replicate tea bags and porewaters were collected several times over one year. TBI decay rates were faster than prior litterbag studies in the same marsh, largely due to rapid green tea loss. Rooibos tea decay rates were more comparable to natural marsh litter, potentially suggesting that is more useful as a standardized organic matter proxy than green tea. Decay was slowest at higher marsh elevations and not consistently related to other biotic (e.g., plants, crab burrows) or abiotic factors (e.g., porewater chemistry), indicating that local hydrology strongly affected organic matter loss rates. TBI rates were 32-118% faster in the 10 cm horizon than at 50 cm. Rates were fastest in the first three months and slowed 54-60% at both depths between 3- and 6- months. Rates slowed further between 6- and 12- months but this was more muted at 10 cm (17%) compared to 50 cm (50%). Slower rates at depth and with time were unlikely due to the TBI stabilization factor, which was similar across depths and decreased from 6 to 12 months. Slower decay at 50 cm demonstrates that rates were constrained by environmental conditions in the deeper horizon rather than the composition of this highly standardized litter. Overall, these patterns suggest that hydrologic setting, which affects oxidant introduction and reactant removal and is often overlooked in marsh decomposition studies, may be a particularly important control on organic matter loss in the short term (3 – 12 months).

1. Introduction

Long term sustainability of salt marshes and their role as a carbon sink depend on efficient preservation of organic matter. Preservation is generally ascribed to a combination of rapid deposition of refractory organic matter and slow decay in anoxic soils (Benner et al., 1991; Morris and Bowden, 1986; Valiela et al., 1985). Yet, variability in soil carbon stocks and accumulation rates within and across marshes indicates that controls on preservation are more complex (Arriola and Cable, 2017; Holmquist et al., 2018). Differential tidal flooding across marsh elevations affects aboveground plant production and the belowground soil environment that, in turn, constrains microbial access to oxidants and organic matter (Guimond & Tamborski, 2021; Morris & Bowden, 1986; Spivak et al., 2019). In surface horizons, marsh plant roots and animal burrows further alter soil structure and chemical gradients that affect organic matter decay, while deeper horizons are generally more stable environments (Gribsholt & Kristensen, 2002; Guimond et al., 2020). Characterizing patterns in organic matter decay across tidal inundation gradients and soil depths may therefore provide a useful framework to assess processes contributing to marsh-scale spatial variability in carbon stocks.

Tidal flooding effects on plant and soil processes are generally strongest along creekbanks and at lower elevations, which are inundated more frequently and for longer relative to interior and higher elevation areas (Guimond & Tamborski, 2021; Howes & Goehringer, 1994; Reed & Cahoon, 1992). Rising and falling tides result in oscillating soil redox conditions, with greater oxygen penetration during emergent periods and more strongly reducing conditions under submergence (Fettrow et al., 2023; Seyfferth et al., 2020; Spivak et al., 2023). Flooding changes the soil environment for decomposition by altering availability of terminal electron acceptors, increasing pore space connectivity, leaching organic matter, and changing microbial access to bioavailable compounds (e.g., sorption, enzyme functionality, molecular configuration) (Bradley and Morris, 1990; Giblin and Howarth, 1984; Liu and Lee, 2006; Morrissey et al., 2014).

Plant and animal effects on soil decomposition are layered on top of this hydrogeomorphic template. The classic parabolic relationship between flooding and plant productivity suggests there is an optimal flooding regime, where productivity and, presumably, root release of oxygen and bioavailable carbon compounds (hereafter, exudates) peak, with elevations above and below receiving fewer inputs into the rhizosphere to fuel soil microbes (Megonigal et al., 1999; Morris et al., 2002; Mueller et al., 2016; Spivak & Reeve, 2015). The physical properties of surficial soils

are also altered by roots and animal burrows which reduce bulk density and allow for greater infiltration of oxygen to anoxic horizons. Bioturbation by animals can strongly affect decay rates in surface soil horizons, by altering redox conditions, producing excreta, and moving organic matter between oxic and anoxic layers (Kostka et al., 2002b; Kristensen et al., 2012). Soils buried below animal burrows and the active rooting zone are more insulated from inputs of oxygen and root exudates and daily tidal oscillations, typically have higher bulk densities, and are more compacted (Turner et al., 2006). This more stable soil environment is likely a key reason that decomposition slows with depth, but attributing causality is complicated by differences in organic matter composition between surface and deeper horizons (Bulseco et al., 2020; Luk et al., 2021; Yousefi Lalimi et al., 2018). Standardized litter approaches offer ways to test controls on organic matter loss across ecological, geomorphic, and spatial gradients while avoiding potential confounding factors of litter composition and preparation.

Decades of field, lab, and theoretical experiments report a wide range of decay rates, but robust relationships with climatic, landscape, and ecological drivers remain difficult to quantify (Charles and Dukes, 2009; Kirwan et al., 2013, 2014; Kirwan and Blum, 2011; Mueller et al., 2016; Noyce et al., 2023; Tang et al., 2023). The diversity of decay rates likely reflects spatial heterogeneity within wetlands as well as the variety of measurement techniques applied over different time scales (Blum, 1993; Kirby & Gosselink, 1976; Luk et al., 2023; Luk et al., 2021; Newell et al., 1989). Litterbags have the advantage of assessing mass loss of local marsh detritus, but this bulk approach lacks sensitivity and results can be difficult to compare across studies due to differences in the use of above- and/or below- ground material and deployment duration and depth, among other factors (Blum and Christian, 2004; Charles and Dukes, 2009; Christian, 1984; Kirwan and Blum, 2011; Windham, 2001). Geochemical approaches describe organic matter loss and transformations (e.g., C content, stable isotopes, thermal reactivity, biomarkers), can be applied over timescales of seasons to centuries (e.g., radiocarbon), and benefit from multiple proxies, but are resource intensive and require specialized instrumentation (e.g., mass spectrometry) (Benner et al. 1984a, Benner et al. 1984b; Benner et al., 1987; Benner et al., 1991; Duddigan et al., 2020; Luk et al., 2023; Luk et al., 2021; Moran et al., 1989).

The Tea Bag Index (TBI) is an alternative approach that has been widely adopted because the standardized method and materials allow for greater comparability between studies; it is cost effective, does not require specialized instrumentation, and can be accomplished within months by

non-experts (Keuskamp et al., 2013; Mueller et al., 2018). However, like all methods, the TBI rests on assumptions. One key assumption is that the decay dynamics and chemical composition of two different litter types (green and rooibos teas) can be integrated to estimate loss of natural detritus that has characteristics of the proxy constituents. The TBI, in effect, applies a simplified two-pool decay model and assumes that the biochemical compositions of both pools are broadly applicable. An assumption of this model is that the decay dynamics of very specific types of terrestrial organic matter (i.e., rooibos and green teas) reasonably approximate those of local plant detritus. Chemical characterization of green and rooibos teas during a 91-day incubation described changes in carbon functional groups that are consistent with decomposition and not dissimilar to natural litter, supporting the TBI approach (Duddigan et al., 2020). However, green tea is rich in tannins which are lost rapidly (Duddigan et al., 2020), raising the question of whether the mechanism is leaching, microbial decomposition, or some combination (Lind et al., 2022). Consequently, comparing decay rates estimated from the TBI with natural local litter is important for determining the applicability of this approach to the target study system.

Here, we aimed to gain insight to spatial and temporal patterns in decomposition by testing how tidal inundation affects organic matter decay rates across soil depths and over time in a salt marsh. We employed the TBI to examine the effects of these environmental gradients on decay without the potential confounding factor of varying organic matter composition. Recognizing potential limitations of the TBI, we extended the prescribed incubation time from 3 to 12 months and compared TBI decay estimates with mass loss rates of rooibos and green teas individually and of local plant detritus. We predicted that TBI decay rates would be fastest in shallower soil horizons and lower marsh elevations, where porewater flushing is greater and tidal flooding is more frequent, respectively, and positively correlated with plant biomass, bioturbation (as crab burrow density), and porewater redox levels. We further predicted that TBI rates would be fastest in the first three months and then decrease over the following nine months, and that this pattern would be more pronounced in shallower compared to deeper horizons. Lastly, we expected that decay rates of rooibos tea and local detritus would be comparable and slower than TBI rates.

2. Methods

2.1 Study site and design

We tested whether TBI decay rates differ within vs. below the rhizosphere of *Spartina alterniflora* marshes within the Georgia Coastal Ecosystems Long-Term Ecological Research (GCE-LTER) domain (31.421°, -81.290°). Total suspended sediment levels are high in the Altamaha River which feeds into the GCE-LTER domain and contributes to salt marsh vertical accretion (Langston et al., 2021; Mariotti et al., 2024). As a result, these minerogenic marshes have lower soil carbon content, porosity, and permeabilities but higher bulk densities compared to organic-rich marshes (Giblin and Howarth, 1984). Tides are semidiurnal with a ~2 m range.

Study plots were established in summer 2019 along a tidal creek, with a total of 23 plots placed at 3 distances from the creekbank edge (creek: 0 m, 7 plots; middle: 4 m, 8 plots; platform: 14 m, 8 plots) that captured a range of marsh surface elevations, from 0.55 to 1.13 m (North American Vertical Datum of 1988, NAVD 88; Fig. 1). Tea bag decay rates and porewater chemistry were measured at two depths (10 and 50 cm) at discrete intervals over one year (July 2019-2020). Soil temperatures were continuously monitored for ~6 months at both depths. This study was conducted alongside Wu et al. (2022), who measured plot elevations, plant and animal community characteristics, and soil shear strength once during summer 2019, which we use to contextualize and interpret our results.

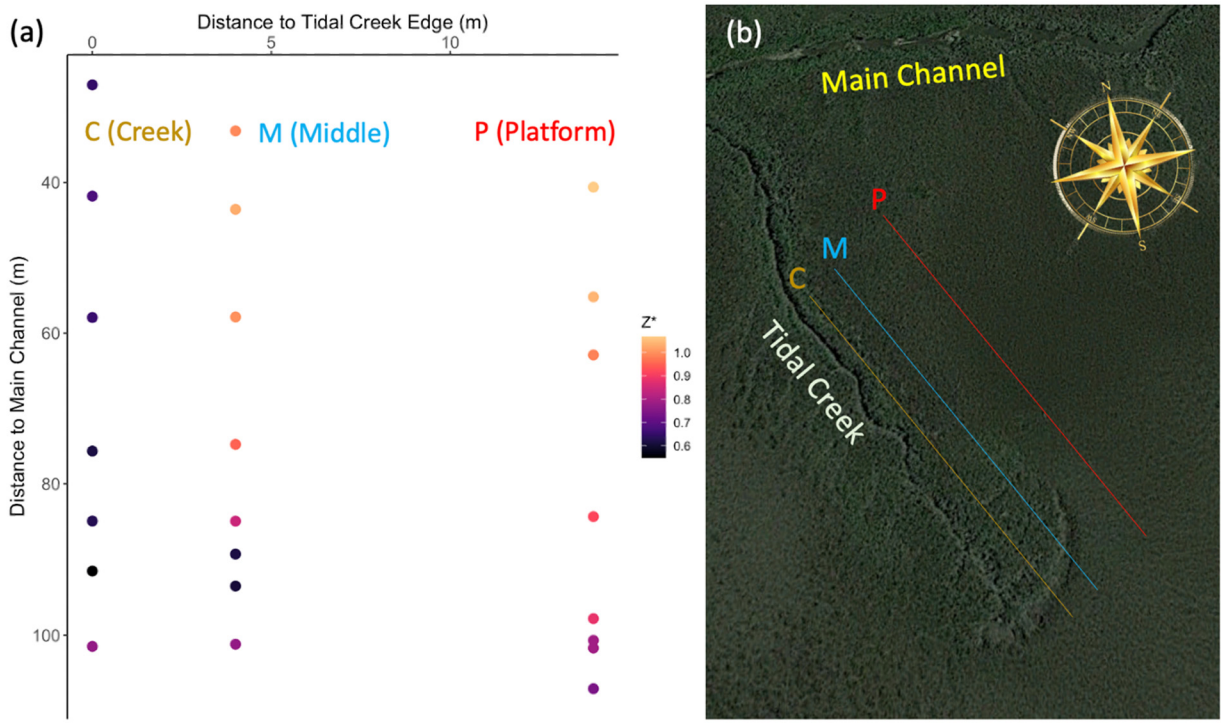

Figure 1. (a) Study plot orientation relative to the main channel, tidal creek, and relative marsh surface elevation (Z*, *see equation 1*). Plots were distributed along the tidal creek (C, 0 m), in the marsh platform (P, 14 m), or in between (M, 4 m) across an elevation range of 0.55-1.13 m (NAVD 88). Plot color corresponds to Z* or relative position in the tidal frame (m). Spacing between plots reflects Wu et al.'s (2022) goal of capturing marsh processes around the fan of a headward eroding creek. (b) Aerial photograph of study site (© Google Earth 2024) with demarcated lines showing approximate plot distribution in respect to the headward eroding creek. Exact plot locations are described by Wu et al. (2022). Plots affected by the headward eroding creek were excluded from this study.

2.2 Marsh Surface Elevation

Marsh surface elevations were measured within 2 m of each plot, to minimize trampling, using a Trimble R6 Real-Time Kinematic Global Positioning System receiver (RTK-GPS; Table S1). The RTK-GPS has a vertical error of ~20 mm. Relative marsh surface elevation of each plot within the tide frame (Z*) was calculated as

$$Z^* = (\text{NAVD88 elevation} - \text{MSL}) / (\text{MHHW} - \text{MSL}), \quad (1)$$

where MSL is mean sea level and MHHW is mean highest high water, referenced to the nearest NOAA tide station (Fort Pulaski, GA 8670870). Elevation data were compared with tide heights, recorded in a nearby creek (31.4437673, -81.2838603), to distinguish between periods of tidal inundation and exposure. Tide heights were recorded in 5-minute intervals by a titanium pressure transducer (Campbell Scientific™ CS456) deployed at a verified elevation and operated by the GCE-LTER project.

2.3 Temperature

Soil temperatures at 10 and 50 cm depths were recorded by HOBO loggers (UA-002-08, Onset Computer Corp, accuracy: ± 0.53° C from 0° to 50° C) in 15-minute intervals. Loggers were intercalibrated prior to deployment (SE ± 0.07° C). The loggers were deployed in July 2019 and collected 188 days (~6 months) later in January 2020. We calculated the average, minimum, and maximum daily temperatures for each of the 15 loggers deployed at 10 cm and the 16 loggers deployed at 50 cm that were recovered and functioning.

2.4 Porewater Chemistry

We collected samples for porewater salinity, pH, and redox in each plot using passive sippers with collection windows at 10 and 50 cm that were deployed in July 2019 (Hughes et al., 2012; Paludan and Morris, 1999). Glass scintillation vials, filled with Milli-Q water (18.2 □□) and fitted with open top caps and 50 □m Nitex mesh, were placed upside down in each collection window. Porewater vials were retrieved two months later and again at 98, 188, and 363 days, which correspond with the 3- , 6-, and 12- month teabag collections. Collected vials were replaced in the sippers with fresh vials and Milli-Q water. Samples were sealed with solid caps and transported on ice to the University of Georgia Marine Institute for measurement. This sampling approach relies on equilibration of water inside the vial with the surrounding porewater, which happens

within one month and was assessed using salinity readings. Salinity was measured with a handheld refractometer while pH levels and redox potential were measured with a benchtop dual channel pH/ISE meter (Fisherbrand™ Accumet™ XL250, accuracy ±0.002 pH units) and a calibrated pH combination electrode (Fisherbrand™ accuTupH™) or redox oxidation / reduction potential electrode (Mettler Toledo™ InLab™ Redox ORP Electrode), respectively. Redox potential readings (mV) were recorded relative to a reference electrode in a 3.5 M potassium chloride solution and values were subsequently corrected to the standard hydrogen electrode.

2.5 Plants, animals, and soil stiffness

Plant characteristics, animal abundances, and soil stiffness were reported previously by Wu et al., 2022. Soil shear strength was measured in the top 4 cm using a field shear vane (GEONOR H-6O). *Spartina alterniflora* aboveground biomass was estimated based on stem density counts and known masses of representative stems. Belowground biomass was measured by collecting soil cores (10 cm diameter, 30 cm depth) centered on a culm of *S. alterniflora* in each plot and then washing roots and rhizomes free of soil before drying and weighing. Two major groups of invertebrates were present: crabs (*Uca pugilator*, *Sesarma reticulatum, Panopeus*) and snails (*Littoraria irrorata*). The densities of burrows (>0.5 cm diameter, all species pooled) and snails (>0.3 cm spire height) were recorded in 0.5 × 0.5 m quadrats at each plot as individuals m^{-2}.

2.6 Decay rates

Decay coefficients (hereafter, rates) were approximated by measuring mass loss over time of a standardized litter. We chose the TBI because this approach has been used broadly across ecosystem types, allowing for intercomparisons (Keuskamp et al., 2013). This method, introduced by Keuskamp et al. (2013), assumes that natural litter is comprised of labile and refractory pools that can be represented by Lipton™ green (European Article Number: 87 22700 05552 5) and rooibos (European Article Number: 87 22700 18843 8) teas, respectively, which we used here. Tea bags were dried at 60 °C to constant mass prior to deployment, during which triplicate bags of each tea type were buried in every plot at 10 and 50 cm depth in July 2019 (initial tea weights: rooibos: 2.01±0.004 g; green: 2.17±0.004 g). Burial depths were chosen to assess decay rates within the more dynamic rhizosphere (10 cm) compared to more stable deeper horizons (50 cm). Single replicates were collected after 98 days (~3 months), 188 days (~6 months), and 363 days

(~12 months, July 2020). Collected tea bags were dried at 60 °C and mass loss was calculated as the difference between the dried initial and final tea masses, after correcting for contributions from the tea bag, string, and label. However, we could not recover all tea bags or use all bags that were recovered due to root ingrowth or other disturbances to integrity of the bags. Such losses were small: fewer than ten tea bags across all 3 times (3-, 6-, and 12- months) and depths (10 and 50 cm) were lost and therefore excluded.

Decay rates were calculated per Keuskamp et al. (2013) using four equations:

$$W(t) = ae^{(-k_1 t)} + (1-a)e^{(-k_2 t)}, \quad (2)$$

$$W(t) = a_r e^{(-kt)} + (1-a_r), \quad (3)$$

$$S = 1 - \frac{a_g}{H_g}, \quad (4)$$

$$a_r = H_r(1-S). \quad (5)$$

Equation 2 combines decay of labile (k_1) and refractory (k_2) organic matter and requires time series data. The TBI eliminates the need for a time series by simplifying equation 2 to equation 3 using the assumptions that decay rates of refractory organic matter are negligible (i.e., $k_2 = 0$) and that the decomposable fraction of organic matter (i.e., a) can be represented by combining different characteristics of rooibos and green teas. In equation 3, $W(t)$ is the mass fraction of rooibos tea remaining at time t, k is the decay coefficient, and S is a stabilization factor. The inhibitory effect of environmental conditions on decay (i.e., S) is calculated based on green tea but assumed to be the same for both tea types. The decomposable fraction (a) of green tea (a_g) is estimated by the mass fraction lost while that of rooibos tea (a_r) is based on its hydrolysable fraction (H_r) and S. We used the tea-specific H values reported by Keuskamp et al. (2013) that were calculated as the sum of nonpolar extractable, water soluble, and acid soluble fractions (H_r: rooibos, 0.552 g g^{-1}; H_g: green, 0.842 g g^{-1}).

We then compared TBI decay rates with tea-specific rates estimated from a first order decay model, which requires time series data:

$$a = a_o e^{(-kt)}, \quad (6)$$

where a is the tea mass fraction remaining after a given amount of time, t, a_o is the initial mass fraction (i.e., 1), and k is the calculated decay coefficient. Single exponential models were fitted to tea-specific mass loss fractions at 0, 98, 188, and 363 days and included 2, 3, or 4 time points, respectively, producing k_g and k_r (Fig. S1). The fraction of variance explained by the decay models

was generally greater for green tea than rooibos. We suspect this is because mass loss rates are a fairly insensitive metric and were much slower for rooibos than green tea. Only models with r^2 values > 0.60 were included for the 6- and 12- month time points to be as representative of the full dataset as possible (i.e., 61% and 100% for the rooibos and green tea bags, respectively). Outliers were removed prior to fitting equation 5 for the 3-month tea bags (see section 2.7). To further assess assumptions of the TBI approach we calculated tea-specific decomposable fractions (a_g and a_r) and stabilization factors (S_g and S_r). Decomposable fractions were defined as mass lost during an incubation and calculated as *1-a*, resulting in a_g (same as Keuskamp et al. 2013) and a_r, for green and rooibos teas, respectively. We used Keuskamp et al.'s (2013) formulation of *S* in equation 3 to represent S_g, but modified it for rooibos tea (S_r) by substituting a_r (decomposable fraction) and H_r:

$$S_r = 1 - \frac{a_r}{H_r}. \qquad (7)$$

From here forward, rates and variables calculated using Keuskamp et al. (2013) or the first order decay approach are referred to TBI and empirical, respectively. For the TBI, this includes TBI k (eq. 3), TBI a_g (fraction mass loss of green tea), TBI a_r (eq. 5), and TBI S (eq. 4) to denote decay rate, the decomposable fractions of green and rooibos teas, and the stabilization factor, respectively. The empirical calculations include k_g and k_r (eq. 6), a_g and a_r (mass fractions lost of each tea type), and S_g (eq. 4) and S_r (eq. 7) where g and r refer to green or rooibos teas, respectively. Importantly, there are two commonalities between these approaches: TBI a_g is the same as empirical a_g, and TBI S is the same as empirical S_g.

2.7 Decay rates from marsh litterbags

Geochemical changes of natural marsh organic matter undergoing decomposition have been well studied in Georgia marshes (Benner et al., 1984b; Benner et al. 1987; Benner et al., 1991; Rice & Tenore, 1981). However, we were unable to find published organic matter mass loss rates from litterbags, which would be a more comparable complement to the TBI. Instead, we draw on a prior experiment conducted June 2003-2004 that used *S. alterniflora* roots collected from the levee and plain of a marsh within GCE-LTER. Decay rates were measured following the methods of Blum (1993) in which 10 g of root material was placed in nylon mesh (2 mm x 2 mm) bags (30 cm x 7 cm) and buried (10 to 20 cm) for 3-to-12 months. Root detritus is a good proxy for evaluating soil organic matter dynamics since this material is deposited directly into anoxic

horizons and contributes to soil accumulation. Sixteen replicates each were initially buried in the marsh levee and plain, and four replicates were retrieved from both sites every ~ 3 months. Bags were transported on ice to the lab and dried at 70° C to constant mass. Decay rates were calculated as in equation 6. Environmental conditions including precipitation and temperature were similar ($p > 0.05$) between the litterbag study in the summer of 2003-2004 (7.7±1.4 cm yr^{-1} and 20.4±2.1 °C) and TBI experiment in the summer of 2019-2020 (12.1±1.9 cm yr^{-1} and 21.4± 2.3 °C)."

2.8 Data analyses

Changes in belowground environmental conditions across marsh surface elevations, between soil depths, and over time were assessed with regression analyses and t-tests. Distance category identity (C, M, P; Fig. 1) was excluded from all statistical analyses because it was confounded with marsh elevation, which we predicted would be a key factor affecting environmental conditions and decay rates. Tidal flooding effects on soil porewater chemistry and temperature were tested by constructing regression models against relative elevation (Z*). Porewater data were then aggregated by sampling event and two sample t-tests were used to detect differences between 10 cm and 50 cm depths. Correlations between Z* and soil temperature were further tested by partitioning according to season (summer: 18/7/2019 to 22/9/2019; fall: 23/9/2019 to 22/12/2019; winter: 23/12/2019 to 19/1/ 2020) and periods of tidal inundation or exposure; differences between slope coefficients were evaluated based on Clogg et al. (1995). We tested whether soil temperatures differed between depths within each season using paired t-tests.

We tested whether decay rates (TBI k, empirical k_g, empirical k_r; d^{-1}) and stabilization factors (TBI S, empirical S_g, empirical S_r) differed over time (3-, 6-, or 12-months) and between soil depths (10 vs 50 cm) by constructing linear mixed effect models using the nlme package for R (Pinheiro et al., 2016). The mixed models evaluated the fixed effects of time and depth and included plot number as a random factor. We then conducted paired t-tests to further explore how TBI and empirical decay rates, decomposable fractions (TBI and empirical a_g and a_r), and stabilization factors changed over time within a depth horizon.

Potential drivers of TBI k were evaluated by calculating Spearman rank correlation coefficients between rates and environmental conditions for the three time points (3, 6, or 12 months) and two soil depths (10 and 50 cm). Porewater data for the 3, 6, and 12 month periods were combined with data from previous time points (e.g., 2, 3, or 6 months) to better represent

cumulative conditions. Temperature was excluded because the shared time series with TBI k violated assumptions of independence. The TBI k values correlated strongly with relative elevation (Z*), *S. alterniflora* rhizome and aboveground biomass, and soil stiffness. We then evaluated interdependencies between these potential drivers by using subsequent single-factor regressions of relative elevation (Z*) vs. aboveground biomass and soil stiffness. Correlations between these variables limited further hypothesis testing of decay drivers to plot position within the tidal frame (Z*). We tested whether TBI k rates and S values changed with relative elevation (Z*) using linear regression models and then evaluated differences between the resulting slope coefficients over time and with depth, as described by Clogg et al. (1995).

Data were tested for outliers using a 1.5 interquartile range cutoff and $\log_{10}$ transformed as needed to meet assumptions of normality. Analyses were conducted using R software (R Development Core Team, 2023. Data are presented as means ± standard error (SE) unless noted otherwise.

3. Results

3.1 Soil porewater chemistry

Porewater chemistry differed between depths and changed over the year but was only weakly sensitive to relative marsh elevation (Z*). Salinities were lower at 10 cm than 50 cm after the first 2 months of the experiment (Fig. 2a) and correlated positively with relative elevation (Z*) at 50 cm (r^2=0.28, $p<0.05$) but not at 10 cm (r^2=0.17, $p>0.05$). Redox potentials were more oxidizing in the shallower horizon and generally decreased over time at both depths but did not vary with relative elevation (Z*) at 10 cm (r^2=0.06, $p>0.05$) or 50 cm (r^2=0.00, $p>0.05$) (Fig. 2b). Porewater pH levels were similar between depths, or slightly higher at 10 cm, with little change over the year (Fig. 2c) and no change with relative marsh elevation (Z*) at either 10 cm (r^2=0.17, $p>0.05$) or 50 cm (r^2=0.15, $p>0.05$).

Temperature differences between 10 and 50 cm were slight (~1 °C) and changed seasonally, with tidal inundation and relative marsh elevation (Z*) (Fig. 3a-f; Table 1). The warmest temperatures were at 10 cm during summer but temperatures were higher at 50 cm in the fall and winter (Table 1A). Soil temperatures were similar across tidal stages in the summer and winter but were warmer during periods of inundation in the fall. Temperatures at 10 cm decreased with increasing relative marsh elevation (Z*) in the summer, regardless of tidal stage, and the fall,

but only during periods of exposure (Fig. 3a, c, f; Table 1B). In contrast, temperatures at 50 cm were less sensitive to marsh elevation within the tidal frame.

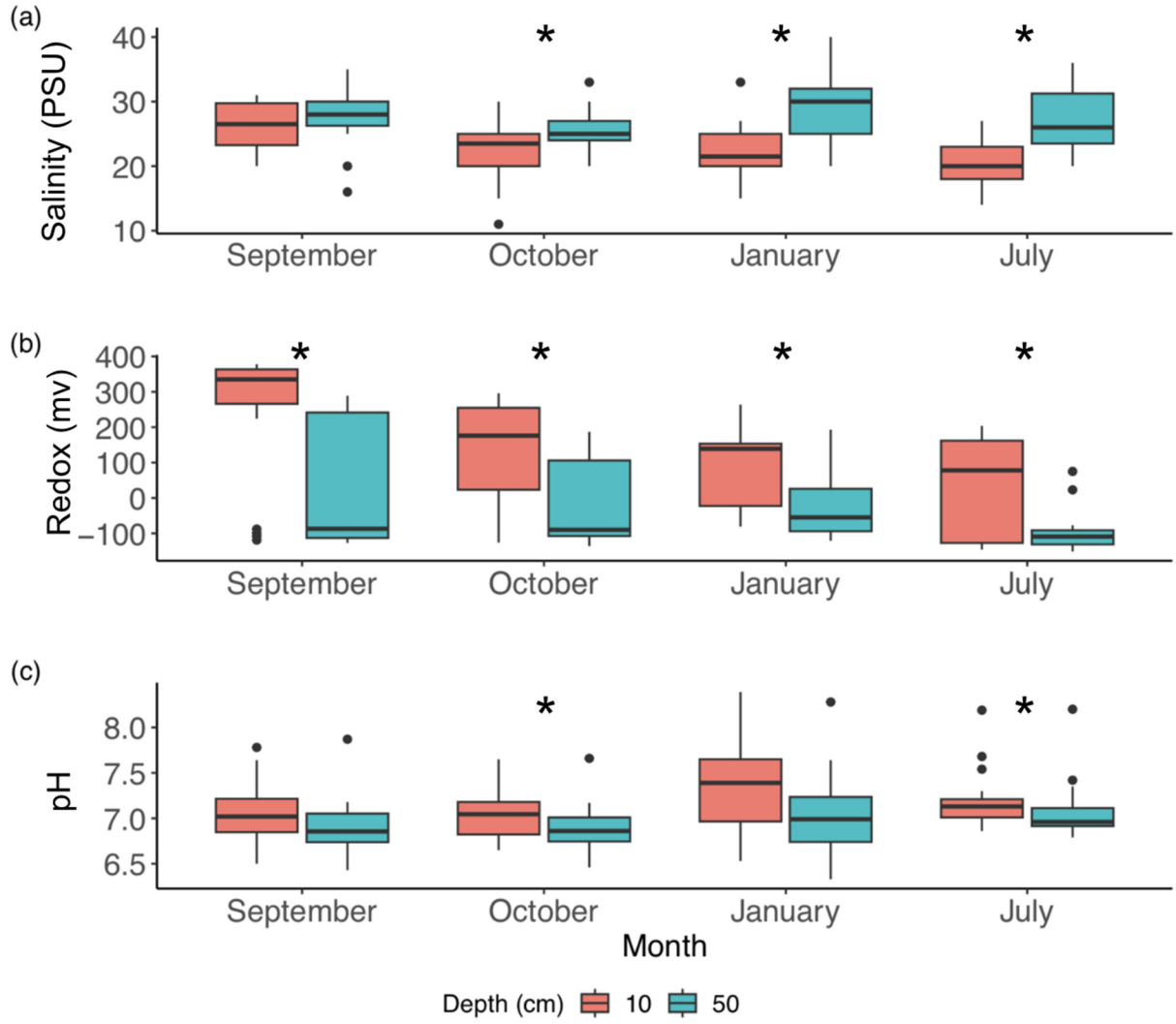

Figure 2. Soil porewater salinity (a), redox (b), and pH (c) pooled across all 23 study plots at 2, 3, 6, and 12 months (September, October, January, and July, respectively) at 10 cm (red) and 50 cm (blue) depths (n=20-23 for each box at each depth). Significant differences ($p<0.05$, as determined by t-tests, see section 2.8) between depths are denoted with an asterisk (*).

Table 1. Soil temperatures by depth and season and with relative position in the tidal frame (Z*). (a). Average (± SE) temperatures (°C) by depth, season, and during periods of tidal inundation or exposure. Significant differences between tidal stages within a season are denoted by * ($p<0.05$) or ** ($p<0.01$) as determined by t-tests; see section 2.8. (b). Linear regression models tested temperature changes with relative marsh surface elevation (Z*) over tidal stages and seasons. Correlations between temperature and relative elevation (Z*) are described by the slope coefficients, associated p values, and the multiple (mult) and adjusted (adj) r^2, that reflect the variance explained by fixed effects alone or by fixed and random effects combined, respectively. Significant differences (<0.05) between tidal stages within a depth and season are denoted by superscripts.

(a)

	10 cm						50 cm					
	Summer		*Fall* **		*Winter* *		*Summer*		*Fall* **		*Winter* *	
	Exposed	Inundated	Exposed	Inundated	Exposed	Inundated	Exposed	Inundated	Exposed	Inundated	Exposed	Inundated
Temp. (°C)	28.19 ± 0.08	28.21 ± 0.06	19.58 ± 0.09	20.95 ± 0.05	15.65 ± 0.06	15.83 ± 0.04	27.25 ± 0.09	27.21 ± 0.09	21.6 ± 0.05	22.57 ± 0.05	16.83 ± 0.04	16.68 ± 0.05

(b)

Depth (cm)	Season	Flooding	Relative Elevation (Z*)		R^2	
			Slope	p-value	Mult. R^2	Adj. R^2
$\log_{10}$ Temp. (°C)						
10 cm	Summer	Exposed	-0.020 ± 0.006 [a]	**0.01**	0.45	0.41
		Inundated	-0.017 ± 0.004 [a]	**0.00**	0.60	0.56
	Fall	Exposed	-0.029 ± 0.011 [a]	**0.02**	0.37	0.32
		Inundated	0.013 ± 0.005 [b]	**0.02**	0.36	0.30
	Winter	Exposed	0.005 ± 0.011 [a]	0.65	0.02	-0.06
		Inundated	-0.011 ± 0.007 [a]	0.15	0.16	0.09
50 cm	Summer	Exposed	-0.012 ± 0.008 [a]	0.16	0.14	0.08
		Inundated	-0.014 ± 0.007 [a]	0.09	0.21	0.15
	Fall	Exposed	-0.009 ± 0.006 [a]	0.16	0.15	0.08
		Inundated	0.013 ± 0.004 [a]	**0.01**	0.45	0.40
	Winter	Exposed	0.007 ± 0.007 [a]	0.30	0.08	0.01
		Inundated	-0.008 ± 0.008 [b]	0.36	0.06	-0.01

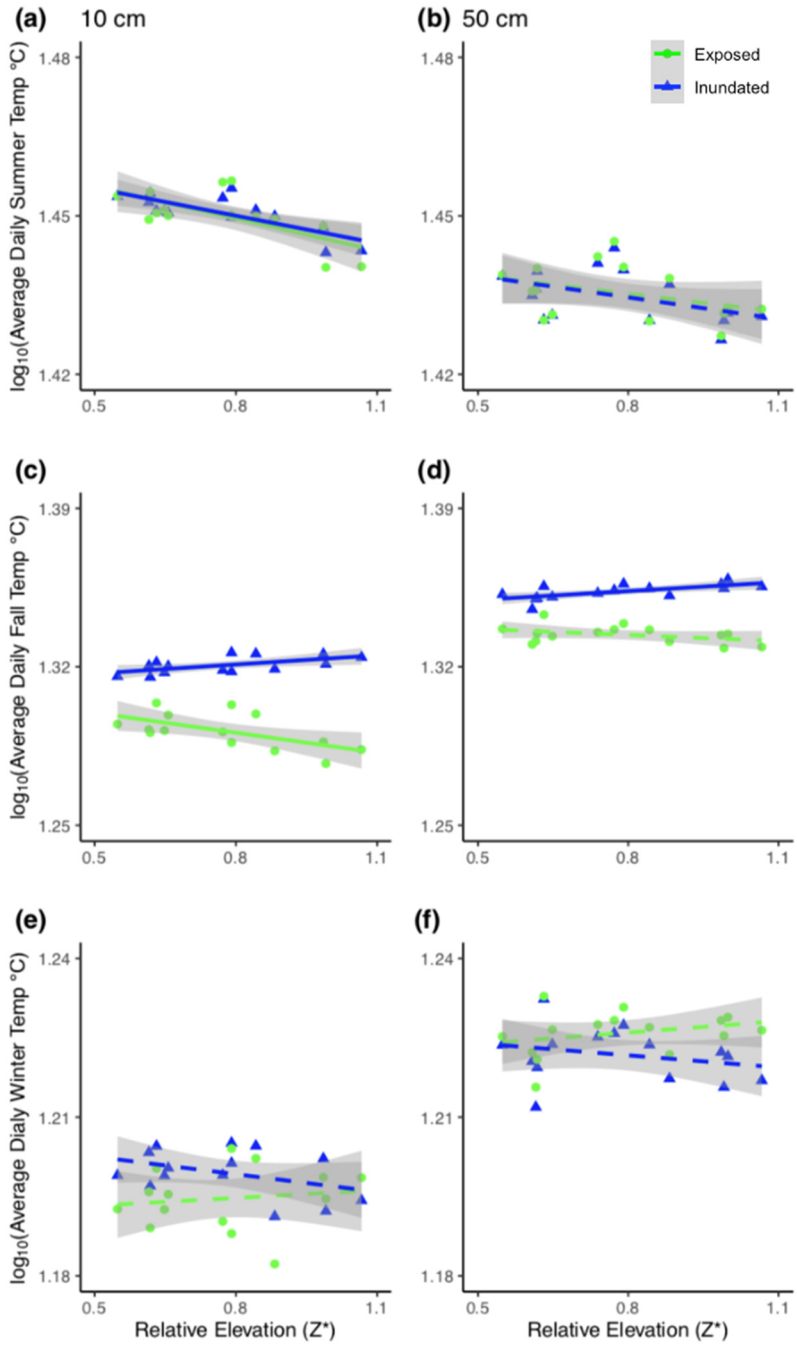

Figure 3. Soil temperatures at 10 cm (left) and 50 cm (right) changed with tidal stage (inundated, blue; exposed, green) and relative mash surface elevation in the tidal frame (Z*) during summer (top), fall (middle), and winter (bottom). Correlations with $p < 0.05$ or > 0.05 are denoted with solid or dashed lines, respectively. See table 1 for statistical results.

3.2 Decay Rates and Stabilization Factors

TBI decay rates (k, d^{-1}) decreased with depth and time (Fig. 4 a, b; Table 3). Rates were 50%, 32%, and 118% faster in the 10 cm horizon at the 3, 6, and 12 month time points, respectively, compared to 50 cm depth. Decay rates slowed to a similar degree between 3 and 6 months at 10 cm (60%) and 50 cm (54%) but there was less of a slowdown between 6 and 12 months at 10 cm (17%) compared to 50 cm (50%; Table 3A). This translated into a 3-fold slowing of turnover times from 140 to 416 days at 10 cm but a 4-fold slowing from 209 to 903 days at 50 cm over the year-long experiment (Table 3A).

Tea-specific empirical decay rates (k_g, k_r) bookended TBI k, differed between burial depths, and changed over time. Green tea rates were 67-162% and 150-327% higher and rooibos tea rates were 48-64% and 34-63% lower at 10 cm and 50 cm, respectively than TBI rates (Fig. 4c-f; Table 3). The percent difference between shallow and deeper rates was much greater for rooibos (29-36%) than green tea (0-2.7%), but both tea types slowed to similar extents at 10 cm and 50 cm between 3-6 months (37-38% green, 39-42% rooibos) and 6-12 months (37-38% green, 34-35% rooibos).

We next compared decomposable fractions (a) and stabilization factors (S) for green and rooibos teas. The TBI and empirical approaches produce the same S and a values for green tea (i.e., TBI S = empirical S_g, TBI a_g = empirical a_g), but not for rooibos (equations 2-5). The TBI a_r values, calculated from H_g and S_g (equation 4), were 71-200% higher than empirical a_r values, based on the mass fraction of rooibos tea lost at each time point and depth (Table 3). Stabilization factors for rooibos tea (empirical S_r) were 247-285% and 279-423% greater than for green tea (TBI S, empirical S_g) at 10 cm and 50 cm, respectively (Table 3). For both tea types S values were lowest at 12 months, but only empirical S_r had lower values at the deeper depth.

Root decay rates estimated from litterbags buried in a nearby *S. alterniflora* marsh ranged from 0.0015-0.0021 d^{-1} and were slightly faster in the interior marsh plain compared to the creekbank levee (Table S2). These rates were slower than decay estimates calculated from the TBI approach and green tea (empirical k_g) but comparable to rooibos tea (empirical k_r) loss rates (Table 3).

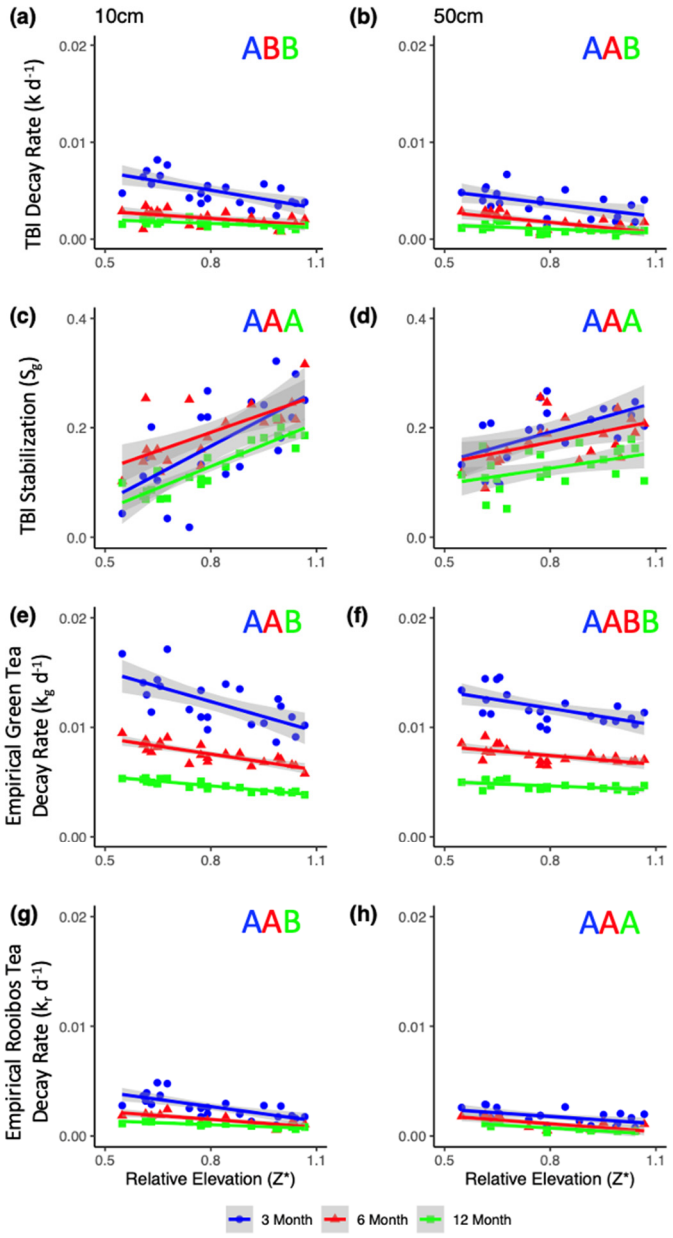

Figure 4. TBI decay rates (a, b) and TBI stabilization factors (c, d) and empirical decay rates (e, f, g, h) at 10 cm (left) and 50 cm (right) and at 3-, 6-, or 12- months (blue, red, and green, respectively). Decay rates decreased while TBI stabilization factors increased with relative marsh surface elevation within the tidal frame (Z*) at both 10 cm and 50 cm depths. Significant correlations ($p<0.05$, as determined by linear regressions, see section 2.8) are denoted with solid lines. Significant differences between linear regressions of TBI k, empirical k_g and k_r, and TBI S with Z* at the different time points are denoted by letters of the same color. See Table 5 for statistical results.

Table 2. Tea bag index (TBI) and empirical decay rates across soil depths and deployment times. Linear mixed effect models were used to test decay and stabilization responses to the depth (10 or 50 cm) and length (3, 6, or 12 months) of deployments. The marginal (mar.) and conditional (cond.) r^2 reflect the variance explained by fixed effects alone or by fixed and random effects combined, respectively. Significant p values (< 0.05) are in bold.

Response	Depth		Time		Depth x Time		R^2	
	Slope	*p*	*Slope*	*p*	*Slope*	*p*	*Mar.*	*Cond.*
TBI k (d^{-1})	$-7.1x10^{-5} \pm 1x10^{-5}$	**<0.001**	$-5.0x10^{-4} \pm 7*10^{-5}$	**<0.001**	$5.3x10^{-6} \pm 2x10^{-6}$	**0.01**	0.35	0.54
Empirical log_{10}(Green k_g (d^{-1}))	$-4.5x10^{-5} \pm 4x10^{-4}$	**0.002**	$-4.3x10^{-2} \pm 2*10^{-3}$	**<0.001**	$-1.3x10^{-5} \pm 5x10^{-5}$	0.80	0.87	0.92
Empirical Rooibos k_r (d^{-1})	$-2.2x10^{-5} \pm 5x10^{-6}$	**<0.001**	$-1.7x10^{-4} \pm 2*10^{-5}$	**<0.001**	$1.1x10^{-6} \pm 7x10^{-7}$	0.10	0.39	0.74
TBI S (same as S_g)	$4.4x10^{-4} \pm 4x10^{-4}$	0.95	$-4.6x10^{-3} \pm 2*10^{-3}$	**<0.001**	$-6.0x10^{-5} \pm 5x10^{-5}$	0.24	0.17	0.47
Rooibos tea stabilization (S_r)	$1.8x10^{-3} \pm 9x10^{-4}$	**<0.001**	$-1.4x10^{-2} \pm 4*10^{-3}$	**<0.001**	$1.7x10^{-4} \pm 1x10^{-4}$	0.12	0.21	0.63

Table 3. Average ± SE of decomposable fractions (a) and stabilization factors used to estimate decay rates (k) and turnover times (days) with the TBI (a) and empirical (b) approaches. Significant differences ($p>0.05$; as determined by t-tests, see section 2.8) between deployment times within a depth horizon are denoted by superscripts.

(a) TBI Calculations

Depth (cm)	Time (months)	a_r	S (or S_g)	k (d^{-1})	Turnover time (d)
10	3	0.46 ± 0.02	0.17 ± 0.02 ^{a}	$7.2*10^{-3} \pm 7*10^{-4}$ ^{a}	140 ± 15
	6	0.45 ± 0.01	0.19 ± 0.01 ^{a}	$2.9*10^{-3} \pm 3*10^{-4}$ ^{b}	341 ± 66
	12	0.48 ± 0.01	0.13 ± 0.01 ^{b}	$2.4*10^{-3} \pm 2*10^{-4}$ ^{b}	416 ± 33
50	3	0.45 ± 0.01	0.19 ± 0.01 ^{a}	$4.8*10^{-3} \pm 5*10^{-4}$ ^{a}	209 ± 33
	6	0.45 ± 0.01	0.18 ± 0.01 ^{a}	$2.2*10^{-3} \pm 3*10^{-4}$ ^{b}	464 ± 105
	12	0.48 ± 0.01	0.13 ± 0.01 ^{b}	$1.1*10^{-3} \pm 9*10^{-5}$ ^{c}	903 ± 115

(b) Empirical Calculations

Tea Type	Depth (cm)	Time (months)	a_r or a_g	S_r	empirical k_g, k_r (d^{-1})	Turnover time (d)
Green	10	3	0.70 ± 0.02^{a}		$1.2*10^{-2} \pm 5*10^{-4}$ ^{a}	85 ± 3
		6	0.68 ± 0.01^{a}		$7.6*10^{-3} \pm 2*10^{-4}$ ^{b}	134 ± 4
		12	0.73 ± 0.01^{b}		$4.7*10^{-3} \pm 1*10^{-4}$ ^{c}	217 ± 5
	50	3	0.68 ± 0.01^{a}		$1.2*10^{-3} \pm 3*10^{-4}$ ^{a}	86 ± 2
		6	0.69 ± 0.01^{a}		$7.4*10^{-3} \pm 2*10^{-4}$ ^{b}	136 ± 3
		12	0.74 ±0.01^{b}		$4.7*10^{-3} \pm 7*10^{-5}$ ^{c}	216 ± 4
Rooibos	10	3	0.22 ± 0.02^{a}	0.59	$2.6*10^{-3} \pm 2*10^{-4}$ ^{a}	440 ± 40
		6	0.18 ± 0.02^{b}	0.68	$1.5*10^{-3} \pm 1*10^{-4}$ ^{b}	785 ± 103
		12	0.28 ± 0.01^{c}	0.50	$9.8*10^{-4} \pm 6*10^{-5}$ ^{c}	1083 ± 75
	50	3	0.16 ± 0.01^{a}	0.72	$1.8*10^{-3} \pm 1*10^{-4}$ ^{a}	697 ± 78
		6	0.15 ± 0.02^{a}	0.74	$1.1*10^{-3} \pm 1*10^{-4}$ ^{b}	1168 ± 165
		12	0.18 ± 0.02^{a}	0.68	$7.3*10^{-4} \pm 1*10^{-4}$ ^{c}	1703 ± 248

3.3 Plants, soil stiffness, and animal communities

Linear regression analyses demonstrated that soil shear strength decreased with increasing relative elevation (Z*; r^2=0.21, p<0.05) (Wu et al. 2022). Plant density did not change across the relative elevation gradient (p > 0.05) while stem height (r^2=0.36, p<0.05) and aboveground biomass (r^2=0.60, p<0.05) both decreased with increasing Z*; Wu et al. 2022). Two major groups of invertebrates were present: crabs (*Uca pugilator*, *Sesarma reticulatum, Panopeus*) and snails (*Littoraria irrorata*) (Wu et al. 2022). Densities of crab burrows and snails were not correlated with relative elevation (Z*; p>0.05).

3.4 Biotic and abiotic variables correlated with TBI decay rates

TBI decay rates (i.e., TBI k) at 10 and 50 cm depth negatively correlated with relative elevation (Z*) across all time points (Table 5). Rates also correlated with other abiotic and biotic factors but, unlike Z*, none of these relationships were consistently significant at both depths and throughout the experiment (Table 4). For instance, porewater salinity correlated with TBI decay at 50 cm, but not 10 cm. Variables reflecting certain plant (stem height, above- and below-ground biomass) and soil (stiffness) characteristics consistently correlated with decay rates at 3- and 6-months but not at 12- months at both depths. Other variables representing bioturbation (crab burrows), grazing (snails) and porewater chemistry (pH, redox) correlated sporadically, if at all, with TBI decay (Table 4). The directionality of many of these correlations (but not statistical significance) remained unchanged over the 12-month period. To explore this further, we evaluated correlations between relative elevation (Z*) and aboveground plant biomass and soil stiffness. Negative relationships with aboveground biomass (r^2 =0.60, p<0.05) point to lower grass production at higher elevations. Positive correlations with soil stiffness (r^2 = 0.21, p<0.05) are consistent with less consolidation (i.e., greater porewater flushing, more root production) or other gradients in soil properties (e.g., grain size, which affects burrowing) at lower elevations. Because plant and soil properties affect decay (Liu et al., 2008; Noyce et al., 2023), and we cannot separate those drivers from relative marsh surface elevation (Z*), we focus on how decay changes with position in the tidal frame from here forward.

Table 4. Spearman rank correlation coefficients between TBI decay rates (TBI k, d^{-1}) and potential abiotic and biotic drivers at 10 and 50 cm depth and for the three deployment intervals (3, 6, or 12 months). Significant correlation coefficients ($p < 0.05$) are denoted by *.

Response	10 cm			50 cm		
	3 mon.	6 mon.	12 mon.	3 mon.	6 mon.	12 mon.
Relative marsh surface elevation (Z*)	-0.60*	-0.52*	-0.64*	-0.49*	-0.58*	-0.44*
Crab burrows (count m^{-2})	-0.27	-0.59*	-0.16	-0.13	-0.43*	-0.32
Snails (ind m^{-2})	-0.30	-0.16	0.33	-0.41	-0.37	-0.23
Spartina stem density (shoots m^{-2})	-0.39	-0.37	0.18	-0.4	-0.53*	-0.41*
Spartina stem height (cm)	0.57*	0.53*	0.09	0.62*	0.80*	0.60*
Spartina aboveground biomass (g m^{-2})	0.54*	0.61*	0.60*	0.46*	0.66*	0.34
Spartina root biomass (g cm^{-3})	0.38	0.22	-0.07	0.22	0.45*	0.12
Spartina rhizome biomass (g cm^{-3})	0.60*	0.45*	0.54*	0.61*	0.58*	0.29
Soil stiffness (kPa)	-0.60*	-0.71*	-0.33	-0.53*	-0.78*	-0.63*
Porewater salinity (PSU)	-0.41	-0.45	-0.15	-0.43*	-0.79*	-0.60*
Porewater pH	0.25	0.57*	0.42	0.42	0.28	0.29
Porewater redox (Eh)	-0.33	0.15	-0.07	0.26	0.32	0.24

3.5 Decay, Stabilization, and Relative Marsh Surface Elevation (i.e., Z*)

TBI and empirical decay rates decreased while TBI S increased at higher relative elevations (Z*; Table 5, Fig.4). Changes in TBI and empirical green tea decay rates with relative elevation (Z*) at 10 cm and 50 cm were sharpest at three months and became less pronounced with time. Further, these gradients were generally steeper at 10 cm and more gradual at 50 cm. In contrast, correlations between relative elevation (Z*) and empirical rooibos decay rates were more similar between soil depths and stable over time. Correlations with relative elevation (Z*) generally accounted for greater fractions of the variability in empirical green (r^2 = 0.44-0.86) and rooibos (r^2 = 0.50-0.75) rates compared to TBI decay (r^2 = 0.33-0.41) at 10 cm. The explanatory power of relative elevation (Z*) was lower at 50 cm for the empirical rates but differences between depths were less clear for TBI rates.

The TBI S factors had the opposite relationship with relative elevation (Z*) and increased at higher elevations but these correlations did not change over time at either 10 or 50 cm depth (Fig. 4c-d; Table 5). The change in TBI S with relative elevation (Z*) was greater at 10 cm compared to 50 cm and these correlations were largely constant throughout the experiment (Table 5).

Table 5. Decay rates (k, d^{-1}) decreased and TBI stabilization factors (S_g) increased relative to marsh surface position in the tidal frame (Z*) at both depths and throughout the experiment. Differences between slopes across the three time points within a depth horizon are denoted by superscripts as determined by the methods of Clogg et al. (1995); see section 2.8.

Response	Depth (cm)	Time (months)	Relative Elevation (Z*)		r^2
			Slope	*P*	
TBI Decay rate ($k\ d^{-1}$)	10	3	$-1.2x10^{-2} \pm 3x10^{-3}$ [a]	<0.01	0.41
		6	$-4.1x10^{-3} \pm 2x10^{-3}$ [b]	0.02	0.27
		12	$-2.6x10^{-3} \pm 8x10^{-4}$ [b]	<0.01	0.33
	50	3	$-6.8x10^{-3} \pm 3x10^{-3}$ [a]	0.02	0.25
		6	$-5.6x10^{-3} \pm 1x10^{-3}$ [a]	<0.01	0.47
		12	$-1.2x10^{-3} \pm 5x10^{-4}$ [b]	0.03	0.24
TBI Stabilization (S_g)	10	3	0.34 ± 0.09 [a]	<0.01	0.43
		6	0.22 ± 0.06 [a]	<0.01	0.48
		12	0.26 ± 0.03 [a]	<0.01	0.82
	50	3	0.18 ± 0.06 [a]	<0.01	0.35
		6	0.13 ± 0.05 [a]	0.02	0.25
		12	0.10 ± 0.04 [a]	0.03	0.21
Empirical Green tea decay ($k_g\ d^{-1}$)	10	3	$-9.2x10^{-3} \pm 2x10^{-3}$ [a]	<0.01	0.44
		6	$-4.9x10^{-3} \pm 7x10^{-4}$ [a]	<0.01	0.68
		12	$-2.8x10^{-3} \pm 3x10^{-4}$ [b]	<0.01	0.86
	50	3	$-5.2x10^{-3} \pm 2x10^{-3}$ [a]	<0.01	0.35
		6	$-2.7x10^{-3} \pm 8x10^{-4}$ [ab]	<0.01	0.38
		12	$-1.3x10^{-3} \pm 4x10^{-4}$ [b]	<0.01	0.34
Empirical Rooibos tea decay ($k_r\ d^{-1}$)	10	3	$-4.4x10^{-3} \pm 1x10^{-3}$ [a]	<0.01	0.50
		6	$-2.4x10^{-3} \pm 5x10^{-4}$ [a]	<0.01	0.67
		12	$-1.2x10^{-3} \pm 2x10^{-4}$ [b]	<0.01	0.75
	50	3	$-2.2x10^{-3} \pm 8x10^{-4}$ [a]	0.01	0.27
		6	$-2.4x10^{-3} \pm 6x10^{-4}$ [a]	<0.01	0.55
		12	$-1.9x10^{-3} \pm 5x10^{-4}$ [a]	<0.01	0.66

4. Discussion

4.1 Methodological considerations.

Decay rates based on the TBI and empirical green and rooibos teas (i.e., k_g, k_r) slowed over time and with depth and were fastest in plots sitting lower in the tidal frame (Fig. 4, Table 3, 5). Average green tea decay rates were 67-327% faster than TBI k which was 34-64% faster than rooibos rates (Table 3). Between soil depths, TBI and rooibos decay rates were 30-118% and 34-44% faster, respectively, at 10 cm compared to 50 cm whereas empirical green tea rates were nearly equivalent (0-3% change; Table 3). Differences between TBI and empirical decay rates at both depths and, for rooibos tea, with time were relatively constant while the gap between TBI and green tea widened over the year. These patterns suggest that, at the plot scale and over one year, TBI rates reflect rooibos tea dynamics (oxidized needles and branches from the rooibos bush) slightly more than green tea (*Camellia sinensis* leaves and buds).

At a larger scale across marsh surface elevations, changes in TBI k with relative elevation (Z*) closely mirrored empirical green tea dynamics, especially in the shallower soil horizon (Table 5; Fig. 4). Steeper drops in TBI decay with relative elevation (Z*) during the first three months were driven by changes in green tea mass loss and likely influenced by leaching due to greater tidal flushing of porewater at lower elevations (Fig. 4, Table 5). In contrast, mass loss rates of rooibos tea changed less across relative marsh surface elevations (Z*) and were more constant over time. These patterns are consistent with a short-term leaching experiment demonstrating faster losses of green tea (10-50%) than rooibos (<5 – 20%) and greater sensitivity to temperature, water turnover, and soil moisture content (Lind et al., 2022). We cannot isolate the magnitude of leaching effects from microbial decomposition since both would have occurred during the first several months. That leaching accelerates decay is not a problem exclusive to the TBI - it also affects interpretation of mass loss rates from litterbags with local detritus (Cotrufo et al., 2010; Gessner et al., 1999; MacDonald et al., 2018; Seelen et al., 2019) - but the potential magnitude of abiotic loss highlights that decay coefficients from 3-month deployments, as prescribed by Keuskamp et al. (2013), should not be interpreted solely as a function of the microbial community. Instead, extending the duration and increasing the number of sampling points of the TBI could result in decay rates that are more representative of microbial processing (Lind et al., 2022; Marley et al., 2019).

Another argument for extending the duration of TBI studies in marshes is that mass loss rates of green tea did not plateau after three months. Green tea mass loss increased by 4.3% at 10 cm and 8.8% at 50 cm over the final nine months of the experiment (Table 3b, a_g values). The fraction of green tea mass loss was never greater than H_g (hydrolysable fraction of green tea) reported by Keuskamp et al. (2013), as has happened in short-term leaching studies (Lind et al., 2022) and forest soils (Mori et al., 2022). As a result, TBI S did not fall below zero, which would have skewed the TBI a_r. Choice of H_r and H_g values is important because the hydrolysable fraction, operationally defined as the sum of nonpolar, water soluble, and acid soluble compounds, is sensitive to methodology (e.g., Mueller et al., 2018) and affects S.

A central tenant of the TBI is that S asymptotes at three months and values are the same for green and rooibos teas (Keuskamp et al., 2013). However, we found that TBI S (equivalent to S_g) and S_r decreased from 3-to-12 months and values were 247-423% higher for rooibos than green tea (Table 3). Moreover, differences between S_g and S_r increased over time. The caveat that S_g and S_r were not equal is not a function of the marsh environment as Mori et al. (2022) also report differences across four temperate forest stands. The assertion that S is the same for green and rooibos teas rests on the assumption that stabilization is controlled by environmental factors (Keuskamp et al., 2013) and independent of compositional differences that affect organic matter-soil interactions (e.g., mineral association, incorporation into aggregates, etc.) and, as a result, decomposition rates (Marschner et al., 2008; Mikutta et al., 2006). Yet, easily degradable non-structural compounds can be preserved over long time scales due to physio-chemical interactions while complex macromolecules are not intrinsically recalcitrant (Dungait et al., 2012; Kallenbach et al., 2016; Mikutta et al., 2006). As such, there appears to be limited theoretical support for S as formulated by the TBI.

Comparisons between TBI and empirical decay rates averaged across plots demonstrate that this index is weighted slightly more by rooibos mass loss rather than being an equal blend of both teas. However, when distributed across the environmental gradient of tidal flooding (i.e., Z*) the different sensitivities of each tea type became more apparent. Faster mass loss rates of green and rooibos teas, which are rich in soluble tannins and aromatic compounds associated with lignin monomers, respectively (Duddigan et al., 2020), in lower relative elevation (Z*) plots are consistent with leaching in the short-term (3- months) and the effects of porewater turnover on decomposition in the longer term (Fig. 4). Running experiments beyond three months and

increasing sampling frequencies will likely allow for better distinctions between leaching and decomposition effects (Duddigan et al., 2020; Lind et al., 2022; Marley et al., 2019). The TBI was developed for terrestrial soils and our results demonstrate that some assumptions need to be carefully assessed when applying this method to saturated, wetland soils. Knowing the different sensitivities of green and rooibos teas to physical, chemical, and biological processes is valuable for interpreting controls on organic matter mass loss rates across environmental gradients and different ecosystems.

4.2 Decay rate context

Organic matter decay rates estimated by the TBI were higher than previous measurements of 0.0010 – 0.0026 d^{-1} from Georgia's minerogenic salt marshes based on field litterbags and laboratory leaching and incubation experiments conducted over 150 – 540 days (Benner et al., 1984b; Benner et al. 1987; Benner et al., 1991; Rice & Tenore, 1981) (Table S2). The slowest rates were based on lignin while faster rates were estimated from losses of structural polysaccharides (cellulose, hemicellulose) or plant tissue mass. The highest decay rate was calculated from polysaccharides in root and rhizome litter (Benner et al., 1991) and was 30-73% faster than root mass loss along creekbank levees (0.0015 d^{-1}) and marsh interiors (0.0020 d^{-1}; Table S2). The TBI rates at three months were 2.8 – 7.2 times faster than prior studies but that drops to roughly double over longer, 6-12 month periods (10 cm horizon only; Table 3; Fig 4), with the exception of the rapid polysaccharide-specific rate (Benner et al., 1991). This is perhaps not surprising since nuclear magnetic resonance (NMR) spectroscopy demonstrates sharp reductions in O-alkyl compounds consistent with carbohydrates and polysaccharides and aromatic compounds consistent with tannins during green tea incubations (Duddigan et al., 2020). Higher TBI rates could also reflect differences in the preparation and processing (e.g., milling, oxidation) of the organic matter filling tea- and litter- bags. While the TBI greatly overestimates decay of natural litter (120%) empirical rooibos mass loss rates are only slightly faster (36%; Table 3; S2). This suggests that rooibos tea may adequately mimic decay dynamics of local litter, depending on study goals, but combining with green tea in the TBI results in accelerated rate estimates.

We expected TBI rates to be faster in our study in subtropical Georgia, USA, compared to higher latitudes based on the metabolic theory of ecology, which predicts that decay rates increase with rising temperatures (Yvon-Durocher et al., 2010), and observations that warming accelerates

loss of labile compounds in soils (Conant et al., 2011; Melillo et al., 2002). To test this, we compared our rates with those from 7 other salt marsh TBI studies that encompass 11 countries and span a latitudinal gradient of 93.7° (-37.7° to 56°; Fig. 5, Table S3) (Mueller et al., 2018, Puppin et al., 2023, Marley et al., 2019, Alsafran et al., 2017, Yousefi Lalimi et al., 2018, Sanderman and Eagle., unpub; Tang et al., 2023). North America accounted for 50% of the observations, and only one observation came from the southern hemisphere. Teabags were buried at 8 cm in most of those studies, per Keuskamp et al. (2013), whereas we used a 10 cm depth. It is unlikely that this slight difference in burial depth skews comparisons since both are within the rooting zone. Marley et al. (2019) used locally sourced tea, rather than the prescribed Lipton brand, but reported that the two were compositionally similar. Potentially more important is that most studies used TBI H_g and TBI H_r values reported by Keuskamp et al. (2013) while Tang et al. (2023) performed different extractions to derive their own estimates of hydrolysable fractions. Differences in H values across studies are relatively minor and would more strongly affect TBI S (stabilization) than TBI k (decay). Our Sapelo Island, GA, 3-month rates were similar to salt marshes in North Carolina, Virginia, Maryland, California, and Massachusetts, USA and Zeijhong Province (ZJ), China (Fig. 5). The lack of a directional trend within these latitudes contrasts with small-to-moderate warming effects on marsh litter decomposition in field experiments (Charles and Dukes, 2009; Tang et al., 2023) and across spatial gradients (Kirwan et al., 2014). The absence of a general latitudinal trend ($p>0.05$, $r^2=0.01$) for 3-month decay rates could reflect interactions within the soil environment that affect decomposition, such as bioturbation, leaching, tidal flushing, redox conditions, salinity, mineral associations (Conant et al., 2011; Craine et al., 2010), and plant species effects such as rooting depth, growth rate, and exudate composition, among other variables (Fettrow et al., 2023; Keiluweit et al., 2015; Seyfferth et al., 2020; Spivak et al., 2023). It is also possible that 3-month rates are more sensitive to leaching than temperature in saturated marsh soils as differences between sampling time points (3-, 6-, or 12- months) are often as great as between latitudes (e.g., Sapelo Island, GA; Schleswig-Holstein (SH), Germany; East Lothian (ELN), Scotland). It is possible that latitudinal trends may become more apparent following longer teabag deployments when microbial processing would be the dominant control on organic matter loss.

The TBI's stabilization factor (S) is meant to represent the process by which labile compounds in green tea become refractory under certain environmental conditions (Keuskamp et

al., 2013) and should increase over time as decay progresses (Marschner et al., 2008; Mikutta et al., 2006). A slight negative correlation between 3-month TBI S and k values (r^2 =0.11, $p<0.05$) across the compiled data from all seven studies supports this prediction (Fig. 5). However, the negative relationship between TBI S and k is not universal across individual studies (Keuskamp et al., 2013; Seelen et al., 2019). In our experiment on Sapelo Island (GA, USA), the highest S values coincided with the fastest decay rates in the first 3 months (Fig. 5). Stabilization values then decreased between 3- and 6- months but there was no overall temporal trend because values increased at 12-months. This variability is not unique to our site; TBI S values decreased and increased at East Lothian (ELN), Scotland and Schleswig-Holstein (SH), Germany, respectively, between 3- and 12- months (Fig. 5). The absence of a clear latitudinal gradient in TBI S values suggests that this proxy is largely insensitive to global-scale temperature gradients (Fig. 5). Yet, this contrasts with Mueller et al. (2018), who reported higher TBI S values at higher latitudes along the North American Atlantic coast. The mixed relationships between TBI S with k and across latitudes could reflect variability in the many physicochemical processes that affect microbial access to and efficient use of organic matter (e.g., mineral association; Georgiou et al., 2024; Tao et al., 2023). This interpretation, though, is caveated our experimental findings and by Mori et al.'s (2022) discussion that green and rooibos teas do not share S values which violates assumptions of the TBI method (Table 3).

Faster decay rates estimated in this study using the TBI method relative to more conventional litterbag and laboratory experiments suggest that these approaches are not interchangeable. It is possible that tea processing, including oxidation and milling into small pieces, increases vulnerability to decomposition and that microbes respond strongly to compositional differences between allochthonous organic matter (i.e., tea) and local marsh detritus. Similar decay rates between rooibos tea and more conventional approaches suggest that this aspect of the TBI could be a reasonable proxy when the experimental goal is to assess drivers independently of site-specific differences in organic matter composition and material preparation. Few studies like ours have directly compared decay rates from the TBI, its components, and more conventional approaches but this would be useful in assessing whether Keuskamp et al.'s (2013) method can be applied broadly, in dry and saturated soils. If rooibos tea decay rates from 6-month and longer deployments are comparable to more conventional approaches, then clearer patterns between marshes and across latitudes may become more apparent.

595

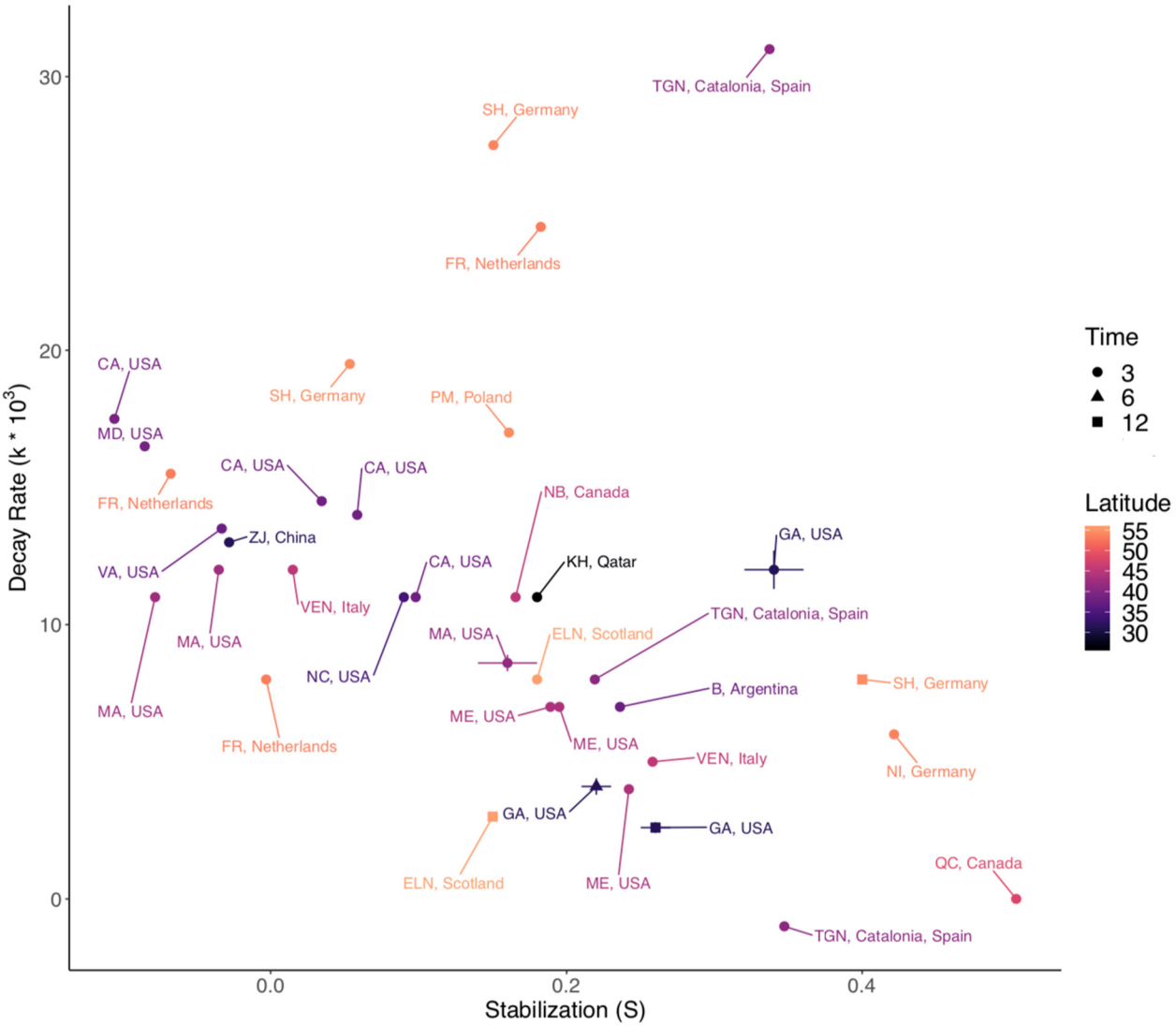

Figure. 5. Average TBI decay rates and stabilization factors in salt marshes as reported by seven data sets spanning a latitudinal gradient of 56.0° N to 37.7° S (see Table S3). To facilitate comparison across northern and southern latitudes all coordinates are represented as positive
600 values. Data are from 3-, 6-, or 12-months of burial at 8-10 cm depth and error bars represent standard error. The GA, USA data are from this study.

4.3 Decay within and below the rhizosphere.

The trajectory of rapid initial TBI decay rates followed by progressive slowing is consistent
605 with decomposition models (Morris and Bowden, 1986; Valiela et al., 1985), litterbags (Benner et al., 1991) and depth profiles of marsh soil organic matter (Luk et al., 2021) and likely reflects

initial losses of soluble and bioavailable compounds and relative accumulation of larger macromolecules (Benner et al., 1991; Marley et al., 2019; Moran et al., 1989; Wilson et al., 1986). Slower rates at deeper depths are consistent with a more stable environment relative to the rhizosphere where root oxygen loss and exudates, bioturbation, and porewater flushing are associated with faster decay (Furukawa et al., 2004; Li et al., 2021; Wilson et al., 2012). However, negative correlations between decay at 50 cm and relative elevation (Z*) demonstrate that deeper soil horizons are not isolated from surface processes.

Faster decay rates during the first 3 months at 10 cm and 50 cm were likely driven by leaching from green and rooibos teas while slower rates in the following nine months may be more representative of microbial decomposition (Duddigan et al., 2020; Lind et al., 2022) (Table 3). The three-month rates may also reflect the summertime deployment since warmer temperatures can accelerate leaching and decay (Kirwan et al., 2014; Lind et al., 2022; Tang et al., 2023). However, seasonality effects are likely small in Georgia where average daily soil temperatures ranged from ~15 to ~ 28 °C between winter and summer (Table 1a). This is narrower than the temperature gradient in an hours-long leaching study that found ~5% and ~10% increases in green tea mass loss between 8 to 19 °C and 19 to 60 °C, respectively (Lind et al., 2022). Microbial decomposition is temperature sensitive (Yvon-Durocher et al., 2010) but responsiveness in wetlands across latitudes and experiments is mixed (Kirwan et al., 2014; Tang et al., 2023). Seasonal changes in plant production and root-microbe interactions also affect decomposition by altering the belowground chemical and physical environment (Van Der Nat et al., 1998; Pett-Ridge et al., 2021). Summertime aboveground and rhizome biomasses and stem height correlated positively with decay, particularly in the first six months, indicating that higher plant abundances correspond to increased TBI mass loss (Table 4). It is unclear whether decay responded to plant-microbe interactions or plant effects on soil structure since correlations were inconsistent at twelve-months (i.e., the following summer). We cannot tease apart temperature effects on leaching and decay further because tea bags were deployed and plants were surveyed only once, during summer. Better assessment of temperature effects on the TBI requires multiple deployments and collections and repeated characterizations of above- and below-ground plant processes across different seasons.

Decay was faster in the top 10 cm, as predicted, but not for the expected reasons (Table 3). We hypothesized that TBI decay and that of green and rooibos teas would be faster in the surface horizon due to greater rhizodeposition, bioturbation, and more oxidizing conditions. Instead, green

tea loss rates were similar at both depths and slower TBI rates at 50 cm were driven by the rooibos tea (Table 3). TBI decay correlated positively with plant characteristics at *both* 10 and 50 cm (Table 4). The rooting zone of *S. alterniflora* extends 20-30 cm and is generally above the 50 cm deployment horizon. Plant effects on soil structure and porewater movement are strongest in the rhizosphere but may extend to deeper depths more weakly, reflecting the year-over-year soil building process and preservation of dead roots and rhizomes. Burrow density did not consistently correlate with TBI decay, but when it did, relationships were negative meaning that rates slowed with more burrowing, which is contrary to most observations (Table 4) (Kostka et al., 2002a; Kostka et al. 2002b; Xiao et al., 2021). Redox conditions were less negative at 10 cm but were not correlated with TBI decay (Fig. 2; Table 4). This was unexpected given thermodynamic constraints of anoxia on decomposition but may be due to loss of compounds that are less redox dependent during the short, one-year incubation whereas decay over longer deployments would become more dependent on processes that are oxygen sensitive, such as depolymerization (Huang et al., 2020; LaCroix et al., 2019). Plant production, bioturbation, redox conditions, and porewater exchange change on time scales of hours-to-seasons and our summertime ecological observations and periodic porewater collections may have been at too coarse a resolution to adequately capture belowground environmental conditions at 10 and 50 cm. Alternatively, the unexpected correlations (or lack thereof) may highlight that many factors influence decay and that short-term rates are more sensitive to other drivers. Regardless, slower rates at 50 cm demonstrate that decay is more constrained by environmental conditions than litter composition, which is consistent with emerging frameworks of organic matter decomposition (Lehmann and Kleber, 2015; Marín-Spiotta et al., 2014; Spivak et al., 2019).

Differences in TBI decay between 10 cm and 50 cm persisted across the relative elevation (Z*) gradient, with faster rates in plots that were lower in the tidal frame (Fig. 4; Table 5). Marsh surface elevation gradients and tidal flooding dictate many aspects of marsh functioning, including plant production and surface soil stiffness which increased and decreased, respectively, in plots at lower relative elevation (Z*) levels. Soil temperatures at 10 cm were warmer at lower marsh surface elevations and differed between inundated and flooded tidal stages, but patterns were less clear and seasonally consistent than in a nearby marsh (Fig. 3; Table 1) (Alber and O'Connell, 2019). Porewater exchange is greater at lower elevations and closer to tidal creeks (Guimond & Tamborski, 2021), which can facilitate decomposition by increasing oxygen delivery to the

subsurface, removing toxic metabolites, increasing pore-space connectivity, and altering organic matter-mineral associations (Canfield, 1989; Liu et al., 2008; Xiao et al., 2021). Sharp changes in TBI rates across the relative elevation (Z*) gradient at three months likely reflect more extensive leaching at lower elevations where soil stiffness is also lower and porewater exchange would be greater (Fig. 4; Tables 4-5) (Guimond & Tamborski, 2021; Lind et al., 2022). This is also consistent with a sharper drop in TBI rates between 3- and 6- months in plots with the lowest relative elevation (Z*) values (Fig. 4a, Table 5). More moderate changes in TBI rates with relative elevation (Z*) at 6- and 12- months indicate that inundation effects on decay extend beyond leaching, which plateaus between 20 (green) and 80 (rooibos) days (Duddigan et al., 2020). Our results contrast with a recent study in Venice Lagoon (Italy) but comparisons are tricky because Puppin et al.'s (2023) analysis combines tea bag burial depth (0-24 cm) with marsh surface elevation into the variable z_{β}, making it difficult to assess those factors independently. Further analyses focused on the shallowest horizon (8 cm) in Puppin et al. (2023) where TBI k slowed with increasing distance from creekbank edges but showed no correlation with estimated time flooded over the 3-month deployment. In our study, it is not possible to differentiate effects of creekbank distance from flooding duration because they were confounded but testing this could provide insight into the sensitivity of decay to soil structure and hydrology. Because inundation influences many ecological, physical, and biogeochemical factors, we cannot definitively attribute correlations between relative elevation (Z*) and TBI decay to any single one or a combination. However, because relative elevation (Z*) was the only variable that consistently correlated with decay at both depths and all three time points, we suspect that gradients in porewater hydrology are particularly important (Table 4). By 12 months the regression slope between TBI decay and relative elevation (Z*) was ~2x's greater at 10 cm compared to 50 cm, demonstrating that rates become less sensitive to inundation at deeper depths and over time. Moreover, the persistence of correlations between TBI decay and relative elevation (Z*) at 50 cm shows connectivity between surface and deeper horizons and that environmental conditions below the rhizosphere that affect organic matter loss are not constant or uniform.

Our results suggest that short-term organic matter decay is less sensitive to its composition than the soil environment and that porewater hydrology may be a particularly important driver. Tea composition is highly standardized, but decay rates were faster at lower relative marsh elevations (Z*) and shallower soil depths (10 cm), which points to the importance of environmental

controls such as tidal flushing on organic matter loss. Rooibos tea decay rates were slightly higher, but comparable, to natural marsh litter and less affected by leaching than green tea and may therefore be a reasonable proxy for organic matter breakdown over certain timescales (Tables 2-5, S2; Fig. 4). It is possible that kinetic (e.g., temperature) and thermodynamic (e.g., redox) controls become more important over longer timescales, after low molecular weight, soluble compounds are lost and decay is more dependent on depolymerization of larger molecules (Conant et al., 2011; Hu et al., 2020). Deployments beginning in different seasons and lasting longer than one year, and perhaps without green tea, could be useful in assessing within-site sensitivity of decay to temperature and how controls on organic matter loss change over time. Similarly, parallel deployments in mineral and organic marshes with similar flooding regimes but different soil properties (e.g., bulk density, porosity, permeabilities, carbon content, etc.) could provide further insight into how the belowground environment affects decay. Pairing organic matter loss rates with geochemical analyses and rates of porewater exchange would be valuable to understand molecular-level changes and explore the roles of physicochemical protection and hydrology.

4.4 Conclusions

In this minerogenic, subtropical salt marsh, the TBI produced faster organic matter decay rates relative to studies using local plant litter. The faster rates were largely due to initial rapid green tea loss and were greatest in the first three months. Placing TBI rates within the context of more traditional approaches is important for assessing the broad applicability of this method and whether changes, such as extending deployment durations and dropping green tea, are warranted. Publishing decay rates of green and rooibos teas alongside the TBI and site-specific literature values is key for evaluating potential method improvements and better identifying generalizable patterns across environmental gradients, such as elevation, flooding, and latitude. We found that rooibos tea produces decay rates comparable to local litter and that rates slow with depth, time, and increasing marsh surface elevation (Tables 2-5, S2; Fig. 4). Because the composition of rooibos tea is similar to natural litter (Duddigan et al., 2020) and preparation is highly standardized, our findings demonstrate that environmental conditions exert stronger controls on short term decay than molecular recalcitrance, which is in line with current theory (Tables 2-4; Fig. 4) (Lehmann and Kleber, 2015; Marín-Spiotta et al., 2014). Slower, steadier rooibos rates at 50 cm suggest that organic matter surviving transit through the rhizosphere may still be vulnerable to decomposition

in deeper more stable soil horizons. Consistent differences in rooibos decay rates across marsh surface elevation gradients (i.e., Z*), and over time and with depth, indicate that local hydrology strongly affects organic matter loss. This variable is often overlooked in marsh decomposition studies but may be more important than kinetic (e.g., temperature) and thermodynamic (e.g., redox) constraints in the short term.

Data availability

All raw data have been submitted to the GCE LTER and electronic data interchange (EDI) data archives and will have been assigned a publicly accessible digital object identifier prior to publication.

Author contributions

The study was designed by S. Reddy, F. Wu, S. Pennings, and A. Spivak. Data collection and sample analyses were performed by S. Reddy, F. Wu, and W. Farrell. S. Reddy and A. Spivak wrote the initial manuscript draft. S. Reddy, F. Wu, W. Farrell, S. Pennings, M. Eagle, J. Sanderman, C. Craft, and A. Spivak contributed to manuscript editing and review.

Competing interests

The authors declare that they have no conflict of interest.

Acknowledgements

We thank D. Smith, G. Giordano, S. Dong, R. Lofgren, and A. Pinsonneault for assistance with field deployments and lab analyses and the Georgia Coastal Ecosystem LTER for project support (OCE-9982133). S. Reddy was supported by the University of Georgia's Center for Undergraduate Research. Spivak was supported by NSF DEB-2121019, Georgia Sea Grant, and the US Coastal Research Program. F. Wu was supported by Natural Science Foundation of Fujian Province (2022J05278) and Marine and Fishery Development Special Fund of Xiamen (23YYST064QCB36). Any use of trade, firm or product names is for descriptive purposes only and does not imply endorsement by the U.S. Government. This manuscript is contribution number 1124 from the University of Georgia Marine Institute.

References

Alber, M., & O'Connell, J. (2019). Elevation Drives Gradients in Surface Soil Temperature Within Salt Marshes. *Geophysical Research Letters*, *46*. https://doi.org/10.1029/2019GL082374

Alsafran, M. H. S. A., Sarneel, J., & Alatalo, J. M. (2017). Variation in plant litter decomposition rates across extreme dry environments in Qatar. *The Arab World Geographer*, *20*(2–3), 252–261.

Arriola, J. M., & Cable, J. E. (2017). Variations in carbon burial and sediment accretion along a tidal creek in a Florida salt marsh. *Limnology and Oceanography*, *62*(S1), S15–S28.

Benner, R., Fogel, M. L., & Sprague, E. K. (1991). Diagenesis of belowground biomass of Spartina alterniflora in salt-marsh sediments. *Limnology and Oceanography*, *36*(7), 1358–1374.

Benner, R., Fogel, M. L., Sprague, E. K., & Hodson, R. E. (1987). Depletion of 13C in lignin and its implications for stable carbon isotope studies. *Nature*, *329*(6141), 708–710.

Benner, R., Maccubbin, A. E., & Hodson, R. E. (1984a). Anaerobic biodegradation of the lignin and polysaccharide components of lignocellulose and synthetic lignin by sediment microflora. *Applied and Environmental Microbiology*, *47*(5), 998–1004.

Benner, R., Newell, S. Y., Maccubbin, A. E., & Hodson, R. E. (1984b). Relative contributions of bacteria and fungi to rates of degradation of lignocellulosic detritus in salt-marsh sediments. *Applied and Environmental Microbiology*, *48*(1), 36–40.

Blum, L. K. (1993). Spartina alterniflora root dynamics in a Virginia marsh. *Marine Ecology-Progress Series*, *102*, 169.

Blum, L. K., & Christian, R. R. (2004). Belowground production and decomposition along a tidal gradient in a Virginia salt marsh. *The Ecogeomorphology of Tidal Marshes*, *59*, 47–73.

Bradley, P. M., & Morris, J. T. (1990). Influence of oxygen and sulfide concentration on nitrogen uptake kinetics in Spartina alterniflora. *Ecology*, *71*(1), 282–287.

Bulseco, A. N., Vineis, J. H., Murphy, A. E., Spivak, A. C., Giblin, A. E., Tucker, J., & Bowen, J. L. (2020). Metagenomics coupled with biogeochemical rates measurements provide evidence that nitrate addition stimulates respiration in salt marsh sediments. *Limnology and Oceanography*, *65*, S321–S339.

Canfield, D. E. (1989). Sulfate reduction and oxic respiration in marine sediments: implications for organic carbon preservation in euxinic environments. *Deep Sea Research Part A. Oceanographic Research Papers*, *36*(1), 121–138.

Charles, H., & Dukes, J. S. (2009). Effects of warming and altered precipitation on plant and nutrient dynamics of a New England salt marsh. *Ecological Applications*, *19*(7), 1758–1773.

Christian, R. R. (1984). A life-table approach to decomposition studies. *Ecology*, *65*(5), 1693–1697.

Clogg, C. C., Petkova, E., & Haritou, A. (1995). Statistical Methods for Comparing Regression Coefficients Between Models. *American Journal of Sociology*, *100*(5), 1261–1293. http://www.jstor.org/stable/2782277

Conant, R. T., Ryan, M. G., Ågren, G. I., Birge, H. E., Davidson, E. A., Eliasson, P. E., Evans, S. E., Frey, S. D., Giardina, C. P., & Hopkins, F. M. (2011). Temperature and soil organic

matter decomposition rates–synthesis of current knowledge and a way forward. *Global Change Biology*, *17*(11), 3392–3404.

Cotrufo, M. F., Ngao, J., Marzaioli, F., & Piermatteo, D. (2010). Inter-comparison of methods for quantifying above-ground leaf litter decomposition rates. *Plant and Soil*, *334*, 365–376.

Craine, J. M., Fierer, N., & McLauchlan, K. K. (2010). Widespread coupling between the rate and temperature sensitivity of organic matter decay. *Nature Geoscience*, *3*(12), 854–857.

Duddigan, S., Shaw, L. J., Alexander, P. D., & Collins, C. D. (2020). Chemical underpinning of the tea bag index: an examination of the decomposition of tea leaves. *Applied and Environmental Soil Science*, *2020*.

Dungait, J. A. J., Hopkins, D. W., Gregory, A. S., & Whitmore, A. P. (2012). Soil organic matter turnover is governed by accessibility not recalcitrance. *Global Change Biology*, *18*(6), 1781–1796.

Fettrow, S., Vargas, R., & Seyfferth, A. L. (2023). Experimentally simulated sea level rise destabilizes carbon-mineral associations in temperate tidal marsh soil. *Biogeochemistry*, *163*(2), 103–120.

Furukawa, Y., Smith, A. C., Kostka, J. E., Watkins, J., & Alexander, C. R. (2004). Quantification of macrobenthic effects on diagenesis using a multicomponent inverse model in salt marsh sediments. *Limnology and Oceanography*, *49*(6), 2058–2072.

Georgiou, K., Koven, C. D., Wieder, W. R., Hartman, M. D., Riley, W. J., Pett-Ridge, J., Bouskill, N. J., Abramoff, R. Z., Slessarev, E. W., & Ahlström, A. (2024). Emergent temperature sensitivity of soil organic carbon driven by mineral associations. *Nature Geoscience*, *17*(3), 205–212.

Gessner, M. O., Chauvet, E., & Dobson, M. (1999). A perspective on leaf litter breakdown in streams. *Oikos*, 377–384.

Google Earth 7.3.6.9796 (2024). *Airport Marsh, Sapelo Island, GA* [Satellite imagery]. Retrieved September 2024, from https://earth.google.com/

Giblin, A. E., & Howarth, R. W. (1984). Porewater evidence for a dynamic sedimentary iron cycle in salt marshes 1. *Limnology and Oceanography*, *29*(1), 47–63.

Gribsholt, B., & Kristensen, E. (2002). Effects of bioturbation and plant roots on salt marsh biogeochemistry: a mesocosm study. *Marine Ecology Progress Series*, *241*, 71–87.

Guimond, J. A., Seyfferth, A. L., Moffett, K. B., & Michael, H. A. (2020). A physical-biogeochemical mechanism for negative feedback between marsh crabs and carbon storage. *Environmental Research Letters*, *15*(3), 034024.

Guimond, J., & Tamborski, J. (2021). Salt marsh hydrogeology: A review. *Water*, *13*(4), 543.

Holmquist, J. R., Windham-Myers, L., Bliss, N., Crooks, S., Morris, J. T., Megonigal, J. P., Troxler, T., Weller, D., Callaway, J., & Drexler, J. (2018). Accuracy and precision of tidal wetland soil carbon mapping in the conterminous United States. *Scientific Reports*, *8*(1), 9478.

Howes, B. L., & Goehringer, D. D. (1994). Porewater drainage and dissolved organic carbon and nutrient losses through the intertidal creekbanks of a New England salt marsh. *Marine Ecology Progress Series. Oldendorf*, *114*(3), 289–301.

Hu, Y., Zheng, Q., Noll, L., Zhang, S., & Wanek, W. (2020). Direct measurement of the in situ decomposition of microbial-derived soil organic matter. *Soil Biology and Biochemistry*, *141*, 107660.

Huang, W., Ye, C., Hockaday, W. C., & Hall, S. J. (2020). Trade-offs in soil carbon protection mechanisms under aerobic and anaerobic conditions. *Global Change Biology*, *26*(6), 3726–3737.

Hughes, A. L. H., Wilson, A. M., & Morris, J. T. (2012). Hydrologic variability in a salt marsh: Assessing the links between drought and acute marsh dieback. *Estuarine, Coastal and Shelf Science*, *111*, 95–106.

Kallenbach, C. M., Frey, S. D., & Grandy, A. S. (2016). Direct evidence for microbial-derived soil organic matter formation and its ecophysiological controls. *Nature Communications*, *7*(1), 13630.

Keiluweit, M., Bougoure, J. J., Nico, P. S., Pett-Ridge, J., Weber, P. K., & Kleber, M. (2015). Mineral protection of soil carbon counteracted by root exudates. *Nature Climate Change*, *5*(6), 588–595.

Keuskamp, J. A., Dingemans, B. J. J., Lehtinen, T., Sarneel, J. M., & Hefting, M. M. (2013). Tea Bag Index: a novel approach to collect uniform decomposition data across ecosystems. *Methods in Ecology and Evolution*, *4*(11), 1070–1075.

Kirby, C. J., & Gosselink, J. G. (1976). Primary production in a Louisiana Gulf Coast Spartina alterniflora marsh. *Ecology*, *57*(5), 1052–1059.

Kirwan, M. L., & Blum, L. K. (2011). Enhanced decomposition offsets enhanced productivity and soil carbon accumulation in coastal wetlands responding to climate change. *Biogeosciences*, *8*(4), 987–993.

Kirwan, M. L., Guntenspergen, G. R., & Langley, J. A. (2014). Temperature sensitivity of organic-matter decay in tidal marshes. *Biogeosciences*, *11*(17), 4801–4808.

Kirwan, M. L., Langley, J. A., Guntenspergen, G., & Megonigal, J. P. (2013). The impact of sea-level rise on organic matter decay rates in Chesapeake Bay brackish tidal marshes. *Kirwan, M. L., Langley, J. A., Guntenspergen, G. R., & Megonigal, J. P. (2013). Biogeosciences,* , *10*(3), 1869–1876.

Kostka, J. E., Gribsholt, B., Petrie, E., Dalton, D., Skelton, H., & Kristensen, E. (2002a). The rates and pathways of carbon oxidation in bioturbated saltmarsh sediments. *Limnology and Oceanography*, *47*(1), 230–240.

Kostka, J. E., Roychoudhury, A., & Van Cappellen, P. (2002b). Rates and controls of anaerobic microbial respiration across spatial and temporal gradients in saltmarsh sediments. *Biogeochemistry*, *60*, 49–76.

Kristensen, E., Penha-Lopes, G., Delefosse, M., Valdemarsen, T., Quintana, C. O., & Banta, G. T. (2012). What is bioturbation? The need for a precise definition for fauna in aquatic sciences. *Marine Ecology Progress Series*, *446*, 285–302.

LaCroix, R. E., Tfaily, M. M., McCreight, M., Jones, M. E., Spokas, L., & Keiluweit, M. (2019). Shifting mineral and redox controls on carbon cycling in seasonally flooded mineral soils. *Biogeosciences*, *16*(13), 2573–2589.

Langston, A. K., Alexander, C. R., Alber, M., & Kirwan, M. L. (2021). Beyond 2100: Elevation capital disguises salt marsh vulnerability to sea-level rise in Georgia, USA. *Estuarine, Coastal and Shelf Science*, *249*, 107093.

Lehmann, J., & Kleber, M. (2015). The contentious nature of soil organic matter. *Nature*, *528*(7580), 60–68.

Li, H., Bölscher, T., Winnick, M., Tfaily, M. M., Cardon, Z. G., & Keiluweit, M. (2021). Simple plant and microbial exudates destabilize mineral-associated organic matter via multiple pathways. *Environmental Science & Technology*, *55*(5), 3389–3398.

Lind, L., Harbicht, A., Bergman, E., Edwartz, J., & Eckstein, R. L. (2022). Effects of initial leaching for estimates of mass loss and microbial decomposition—Call for an increased nuance. *Ecology and Evolution*, *12*(8), e9118.

Liu, Z., & Lee, C. (2006). Drying effects on sorption capacity of coastal sediment: The importance of architecture and polarity of organic matter. *Geochimica et Cosmochimica Acta*, *70*(13), 3313–3324.

Liu, Z., Lee, C., & Aller, R. C. (2008). Drying effects on decomposition of salt marsh sediment and on lysine sorption. *Journal of Marine Research*, *66*(5), 665–689.

Luk, S., Eagle, M. J., Mariotti, G., Gosselin, K., Sanderman, J., & Spivak, A. C. (2023). Peat decomposition and erosion contribute to pond deepening in a temperate salt marsh. *Journal of Geophysical Research: Biogeosciences*, *128*(2), e2022JG007063.

Luk, S. Y., Todd-Brown, K., Eagle, M., McNichol, A. P., Sanderman, J., Gosselin, K., & Spivak, A. C. (2021). Soil organic carbon development and turnover in natural and disturbed salt marsh environments. *Geophysical Research Letters*, *48*(2), e2020GL090287.

MacDonald, E., Brummell, M. E., Bieniada, A., Elliot, J., Engering, A., Gauthier, T.-L., Saraswati, S., Touchette, S., Tourmel-Courchesne, L., & Strack, M. (2018). Using the Tea Bag Index to characterize decomposition rates in restored peatlands. *Boreal Environment Research*.

Marín-Spiotta, E., Gruley, K. E., Crawford, J., Atkinson, E. E., Miesel, J. R., Greene, S., Cardona-Correa, C., & Spencer, R. G. M. (2014). Paradigm shifts in soil organic matter research affect interpretations of aquatic carbon cycling: transcending disciplinary and ecosystem boundaries. *Biogeochemistry*, *117*, 279–297.

Mariotti, G., Ceccherini, G., Alexander, C. R., & Spivak, A. C. (2024). Centennial changes of salt marsh area in Coastal Georgia (USA) related to large-scale sediment dynamics by river, waves, and tides. *Estuaries and Coasts*, *47*(6), 1498–1516.

Marley, A. R. G., Smeaton, C., & Austin, W. E. N. (2019). An assessment of the tea bag index method as a proxy for organic matter decomposition in intertidal environments. *Journal of Geophysical Research: Biogeosciences*, *124*(10), 2991–3004.

Marschner, B., Brodowski, S., Dreves, A., Gleixner, G., Gude, A., Grootes, P. M., Hamer, U., Heim, A., Jandl, G., & Ji, R. (2008). How relevant is recalcitrance for the stabilization of organic matter in soils? *Journal of Plant Nutrition and Soil Science*, *171*(1), 91–110.

Megonigal, J. P., Whalen, S. C., Tissue, D. T., Bovard, B. D., Allen, A. S., & Albert, D. B. (1999). A plant-soil-atmosphere microcosm for tracing radiocarbon from photosynthesis through methanogenesis. *Soil Science Society of America Journal*, *63*(3), 665–671.

Melillo, J. M., Steudler, P. A., Aber, J. D., Newkirk, K., Lux, H., Bowles, F. P., Catricala, C., Magill, A., Ahrens, T., & Morrisseau, S. (2002). Soil warming and carbon-cycle feedbacks to the climate system. *Science*, *298*(5601), 2173–2176.

Mikutta, R., Kleber, M., Torn, M. S., & Jahn, R. (2006). Stabilization of soil organic matter: association with minerals or chemical recalcitrance? *Biogeochemistry*, *77*, 25–56.

Moran, M. A., Benner, R., & Hodson, R. E. (1989). Kinetics of microbial degradation of vascular plant material in two wetland ecosystems. *Oecologia*, 158–167.

Mori, T., Nakamura, R., & Aoyagi, R. (2022). Risk of misinterpreting the Tea Bag Index: Field observations and a random simulation. *Ecological Research*, *37*(3), 381–389.

Morris, J. T., & Bowden, W. B. (1986). A mechanistic, numerical model of sedimentation, mineralization, and decomposition for marsh sediments. *Soil Science Society of America Journal*, *50*(1), 96–105.

Morris, J. T., Sundareshwar, P. V, Nietch, C. T., Kjerfve, B., & Cahoon, D. R. (2002). Responses of coastal wetlands to rising sea level. *Ecology*, *83*(10), 2869–2877.

Morrissey, E. M., Gillespie, J. L., Morina, J. C., & Franklin, R. B. (2014). Salinity affects microbial activity and soil organic matter content in tidal wetlands. *Global Change Biology*, *20*(4), 1351–1362.

Mueller, P., Jensen, K., & Megonigal, J. P. (2016). Plants mediate soil organic matter decomposition in response to sea level rise. *Global Change Biology*, *22*(1), 404–414.

Mueller, P., Schile-Beers, L. M., Mozdzer, T. J., Chmura, G. L., Dinter, T., Kuzyakov, Y., de Groot, A. V, Esselink, P., Smit, C., & D'Alpaos, A. (2018). Global-change effects on early-stage decomposition processes in tidal wetlands–implications from a global survey using standardized litter. *Biogeosciences*, *15*(10), 3189–3202.

Newell, S. Y., Fallon, R. D., & Miller, J. D. (1989). Decomposition and microbial dynamics for standing, naturally positioned leaves of the salt-marsh grass Spartina alterniflora. *Marine Biology*, *101*, 471–481.

Noyce, G. L., Smith, A. J., Kirwan, M. L., Rich, R. L., & Megonigal, J. P. (2023). Oxygen priming induced by elevated CO2 reduces carbon accumulation and methane emissions in coastal wetlands. *Nature Geoscience*, *16*(1), 63–68.

Paludan, C., & Morris, J. T. (1999). Distribution and speciation of phosphorus along a salinity gradient in intertidal marsh sediments. *Biogeochemistry*, *45*, 197–221.

Pett-Ridge, J., Shi, S., Estera-Molina, K., Nuccio, E., Yuan, M., Rijkers, R., Swenson, T., Zhalnina, K., Northen, T., & Zhou, J. (2021). Rhizosphere carbon turnover from cradle to grave: The role of microbe–plant interactions. *Rhizosphere Biology: Interactions between Microbes and Plants*, 51–73.

Pinheiro, J., Bates, D., DebRoy, S., Sarkar, D., & Team, R. C. (2016). nlme: Linear and nonlinear mixed effects models. *R Package [Code]*, *3*, 1–128.

Puppin, A., Roner, M., Finotello, A., Ghinassi, M., Tommasini, L., Marani, M., & D'Alpaos, A. (2023). Analysis of Organic Matter Decomposition in the Salt Marshes of the Venice Lagoon (Italy) Using Standard Litter Bags. *Journal of Geophysical Research: Biogeosciences*, *128*(6), e2022JG007289.

R Development Core Team: R: A language and environment for statistical computing, R Foundation for Statistical Computing [code]. (2023).

Reed, D. J., & Cahoon, D. R. (1992). The relationship between marsh surface topography, hydroperiod, and growth of Spartina alterniflora in a deteriorating Louisiana salt marsh. *Journal of Coastal Research*, 77–87.

Rice, D. L., & Tenore, K. R. (1981). Dynamics of carbon and nitrogen during the decomposition of detritus derived from estuarine macrophytes. *Estuarine, Coastal and Shelf Science*, *13*(6), 681–690.

Seelen, L. M. S., Flaim, G., Keuskamp, J., Teurlincx, S., Font, R. A., Tolunay, D., Fránková, M., Šumberová, K., Temponeras, M., & Lenhardt, M. (2019). An affordable and reliable assessment of aquatic decomposition: Tailoring the Tea Bag Index to surface waters. *Water Research*, *151*, 31–43.

Seyfferth, A. L., Bothfeld, F., Vargas, R., Stuckey, J. W., Wang, J., Kearns, K., Michael, H. A., Guimond, J., Yu, X., & Sparks, D. L. (2020). Spatial and temporal heterogeneity of geochemical controls on carbon cycling in a tidal salt marsh. *Geochimica et Cosmochimica Acta*, *282*, 1–18.

Spivak, A. C., Pinsonneault, A. J., Hintz, C., Brandes, J., & Megonigal, J. P. (2023). Ephemeral microbial responses to pulses of bioavailable carbon in oxic and anoxic salt marsh soils. *Soil Biology and Biochemistry*, *185*, 109157.

Spivak, A. C., & Reeve, J. (2015). Rapid cycling of recently fixed carbon in a Spartina alterniflora system: a stable isotope tracer experiment. *Biogeochemistry*, *125*, 97–114.

Spivak, A. C., Sanderman, J., Bowen, J. L., Canuel, E. A., & Hopkinson, C. S. (2019). Global-change controls on soil-carbon accumulation and loss in coastal vegetated ecosystems. *Nature Geoscience*, *12*(9), 685–692.

Tang, H., Nolte, S., Jensen, K., Rich, R., Mittmann-Goetsch, J., & Mueller, P. (2023). Warming accelerates belowground litter turnover in salt marshes–insights from a Tea Bag Index study. *Biogeosciences*, *20*(10), 1925–1935.

Tao, F., Huang, Y., Hungate, B. A., Manzoni, S., Frey, S. D., Schmidt, M. W. I., Reichstein, M., Carvalhais, N., Ciais, P., & Jiang, L. (2023). Microbial carbon use efficiency promotes global soil carbon storage. *Nature*, *618*(7967), 981–985.

Turner, R. E., Milan, C. S., & Swenson, E. M. (2006). Recent volumetric changes in salt marsh soils. *Estuarine, Coastal and Shelf Science*, *69*(3–4), 352–359.

Valiela, I., Teal, J. M., Allen, S. D., Van Etten, R., Goehringer, D., & Volkmann, S. (1985). Decomposition in salt marsh ecosystems: the phases and major factors affecting disappearance of above-ground organic matter. *Journal of Experimental Marine Biology and Ecology*, *89*(1), 29–54.

Van Der Nat, F.-F. W. A., Middelburg*, J. J., Van Meteren, D., & Wielemakers, A. (1998). Diel methane emission patterns from Scirpus lacustris and Phragmites australis. *Biogeochemistry*, *41*, 1–22.

Wilson, C. A., Hughes, Z. J., & FitzGerald, D. M. (2012). The effects of crab bioturbation on Mid-Atlantic saltmarsh tidal creek extension: Geotechnical and geochemical changes. *Estuarine, Coastal and Shelf Science*, *106*, 33–44.

Wilson, J. O., Valiela, I., & Swain, T. (1986). Carbohydrate dynamics during decay of litter of Spartina alterniflora. *Marine Biology*, *92*, 277–284.

Windham, L. (2001). Comparison of biomass production and decomposition between Phragmites australis (common reed) and Spartina patens (salt hay grass) in brackish tidal marshes of New Jersey, USA. *Wetlands*, *21*(2), 179–188.

Wu, F., Pennings, S. C., Ortals, C., Ruiz, J., Farrell, W. R., McNichol, S. M., Angelini, C., Spivak, A. C., Alber, M., & Tong, C. (2022). Disturbance is complicated: Headward-eroding saltmarsh creeks produce multiple responses and recovery trajectories. *Limnology and Oceanography*, *67*, S86–S100.

Xiao, K., Wilson, A. M., Li, H., Santos, I. R., Tamborski, J., Smith, E., Lang, S. Q., Zheng, C., Luo, X., & Lu, M. (2021). Large CO2 release and tidal flushing in salt marsh crab burrows reduce the potential for blue carbon sequestration. *Limnology and Oceanography*, *66*(1), 14–29.

Yousefi Lalimi, F., Silvestri, S., D'Alpaos, A., Roner, M., & Marani, M. (2018). The spatial variability of organic matter and decomposition processes at the marsh scale. *Journal of Geophysical Research: Biogeosciences*, *123*(12), 3713–3727.

Yvon-Durocher, G., Jones, J. I., Trimmer, M., Woodward, G., & Montoya, J. M. (2010). Warming alters the metabolic balance of ecosystems. *Philosophical Transactions of the Royal Society B: Biological Sciences*, *365*(1549), 2117–2126.